Variable Star and Exoplanet Section of Czech Astronomical Society and Brno Observatory and Planetarium

Proceedings of the 46th Conference on Variable Stars Research

Europe Training Centre YMCA, Litomyšl, Czech Republic, EU

12th – 14th September 2014

Editor-in-chief **Radek Kocián**

Participants of the conference

TABLE OF CONTENTS

AG Draconis – a symbiotic mystery 4
R.GÁLIS, L.HRIC, L.ŠMELCER

Blazhko effect at the time of *Kepler* 10
M.SKARKA

Flares in eclipsing binary GJ 3236 Cas 14
L.ŠMELCER

FRAM telescope – monitoring of atmospheric extinction and variable star photometry 19
J.JURYŠEK, K.HOŇKOVÁ, M.MAŠEK

New Variable Stars in SvkV Catalogue 23
M.VRAŠŤÁK

Observing RR Lyrae type stars 36
M.SKARKA, J.LIŠKA, R.DŘEVĚNÝ, R.F.AUER

O-C diagrams and period changes in stellar systems 38
J.LIŠKA, M.SKARKA

INTRODUCTION

In September 2014, the Variable Star and Exoplanet Section of Czech Astronomical Society organized traditional autumn conference on research and news in the field of variable stars. The conference was held to commemorate the centenary of the Zdenek Kopal birth in his hometown Litomyšl. Our meeting followed the international conference "Living Together: Planets, Stars and Host Binaries", which was dedicated to the work of Zdenek Kopal in the field of eclipsing binaries.

I want to thank all conference participants, and all speakers for their presented contributions. I also want to thank the Director of the European Training Centre Mrs. Mackova for providing venues for conferences and helpfulness to our needs.

Ladislav Šmelcer
president of Variable Star and Exoplanet
Section of Czech Astronomical Society
Valašské Meziříčí, Januar 09st 2015

NOTES

The scientific content of the proceedings contributions was not reviewed by the OEJV editorial board.

OPEN EUROPEAN JOURNAL ON VARIABLE STARS
September 2014 http://var.astro.cz/oejv ISSN 1801-5964

AG Draconis – a symbiotic mystery

R. GÁLIS [1], L. HRIC [2], L. ŠMELCER [3]

(1) Department of Theoretical Physics and Astrophysics, Institute of Physics, Faculty of Science, P. J. Šafárik University, Park Angelinum 9, 040 01 Košice, Slovakia, rudolf.galis@upjs.sk
(2) Astronomical Institute of the Slovak Academy of Sciences, 059 60 Tatranská Lomnica, Slovakia, hric@ta3.sk
(3) Observatory Valašské Meziříčí, Vsetínská 78, 757 01, Czech Republic, lsmelcer@astrovm.cz

Abstract: Symbiotic system AG Draconis regularly undergoes quiescent and active stages which consist of the series of individual outbursts. The period analysis of new and historical photometric data, as well as radial velocities, confirmed the presence of the two periods. The longer one (~ 550 d) is related to the orbital motion and the shorter one (~ 355 d) could be due to pulsation of the cool component of AG Dra. In addition, the active stages change distinctively, but the outbursts are repeated with periods from 359 - 375 d.

Abstrakt: Na svetelnej krivke symbiotického systému AG Draconis možno rozlíšiť obdobia kľudu a aktivity, ktoré sú charakterizované sériami jednotlivých vzplanutí. Periódová analýza nových a historických fotometrických dát, ako aj meraní radiálnych rýchlostí potvrdila prítomnosť variácií s dvomi periódami: dlhšia (~ 550 d) súvisí s orbitálnym pohybom dvojhviezdy, kratšia (~ 350 d) by mohla byť spôsobená pulzáciami chladnej zložky AG Dra. Zatiaľ čo aktívne obdobia sa navzájom výrazne líšia, jednotlivé vzplanutia sa opakujú s periódou v intervale 359 - 375 d.

Introduction

AG Dra is one of the best studied symbiotic systems. The cool component of AG Dra is of a relatively early spectral type (K0 - K4), low metallicity (Smith et al. 1996) and higher luminosity than that of standard class III. The hot component of AG Dra is considered to be a white dwarf sustaining a high luminosity ($\sim 10^3$ $L_\odot$) and temperature ($\sim 10^5$ K) due to the thermonuclear burning of accreted matter on its surface (Mikolajewska et al. 1995). The radius of the giant was estimated to be ~ 35 $R_\odot$ by Zamanov et al. (2007) and Garcia (1986) found an orbital separation of 400 $R_\odot$. Therefore, the accretion most likely takes place from the stellar wind of the cool giant. Both components are in a circumbinary nebula, partially ionized by the white dwarf.

AG Dra undergoes characteristic symbiotic activity with alternating quiescent and active stages. The latter ones consist of the series of individual outbursts repeating at about a one-year interval. The nature of these periodical outbursts has been a matter of long-term debate. While there is general agreement that the orbital period of AG Dra is about 550 d (Meinunger et al. 1979, Gális et al. 1999), there are variations on shorter time-scales (350 - 380 d) presented by Bastian (1998), Friedjung et al. (2003) and Formiggini & Leibowitz (2012). Understanding the nature and mechanism of this variability is crucial in order to explain the outburst activity of AG Dra and other classical symbiotic stars.

Observations and analysis

We use all available photometry and radial velocities for the study of AG Dra. The new photoelectric and CCD observational material (*U, B, V* and ΔR_i) was obtained at the observatories at Skalnaté Pleso, Stará Lesná and Valašské Meziříčí. Period analysis of the observational data was performed using an advanced implementation of the Date-Compensated Discrete Fourier Transform. We used a Fisher Randomization Test for determining the significance of the obtained periods. The minimum error of period *P* was determined by calculating a 1σ confidence interval on *P*, using the method described by Schwarzenberg-Czerny (1991).

The light curve between the years 1890 and 1966

The historical LC of AG Dra over the period 1889 – 1966 was constructed using the compilation of photographic observations by Robinson (1969). During the period (1890 - 1966), the AG Dra system underwent three phases of activity: the first one between the years 1932 and 1939 (A), the second one between 1949 and 1955 (B) and the third one between 1963 and 1966 (C in Fig. 1). In total, we recognized 15 outbursts in this period.

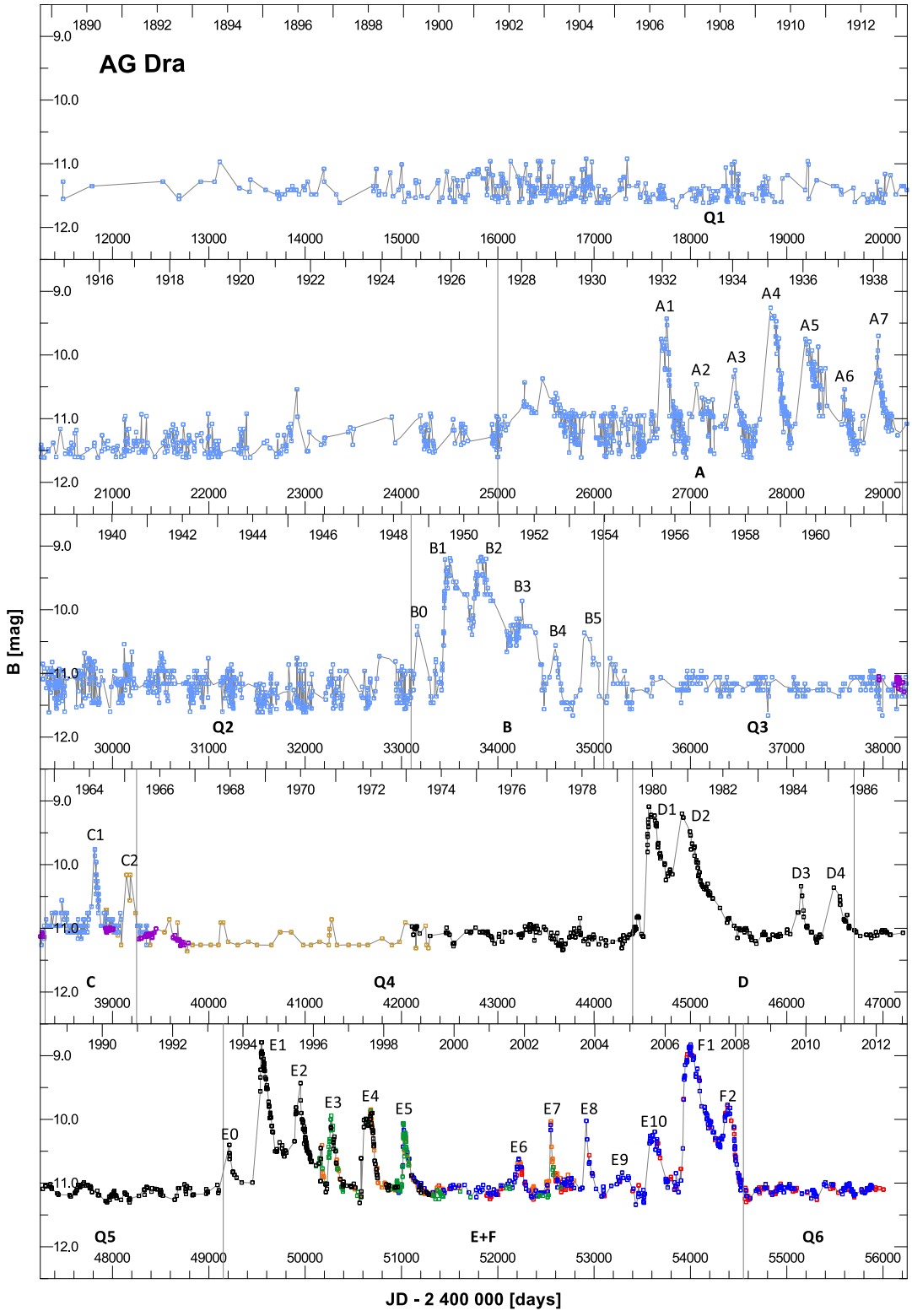

Figure 1: The historical LC of AG Dra over the period 1889 - 2012, constructed on the basis of photographic and *B* photoelectric observations. The LC is divided into active (A - F) and quiescence (Q1 - Q6) stages by vertical lines. Particular outbursts are assigned as A1 - A7, B0 - B5, C1 - C2, D1 - D5, E0 - E10 and F1, F2. The thin curves show spline fits to the data points.

We present the results of this analysis for the given stages in Fig. 2 (left panel). We conclude that the historical LC shows both known periods: ~ 550 d (orbital period) and ~ 350 d (the period of the postulated pulsation of the red giant: Gális et al. 1999). Besides these periods, the analysis gave us the period 370 - 380 d, which is present in the active stages A and C. This period is related to the recurrence of the individual outbursts.

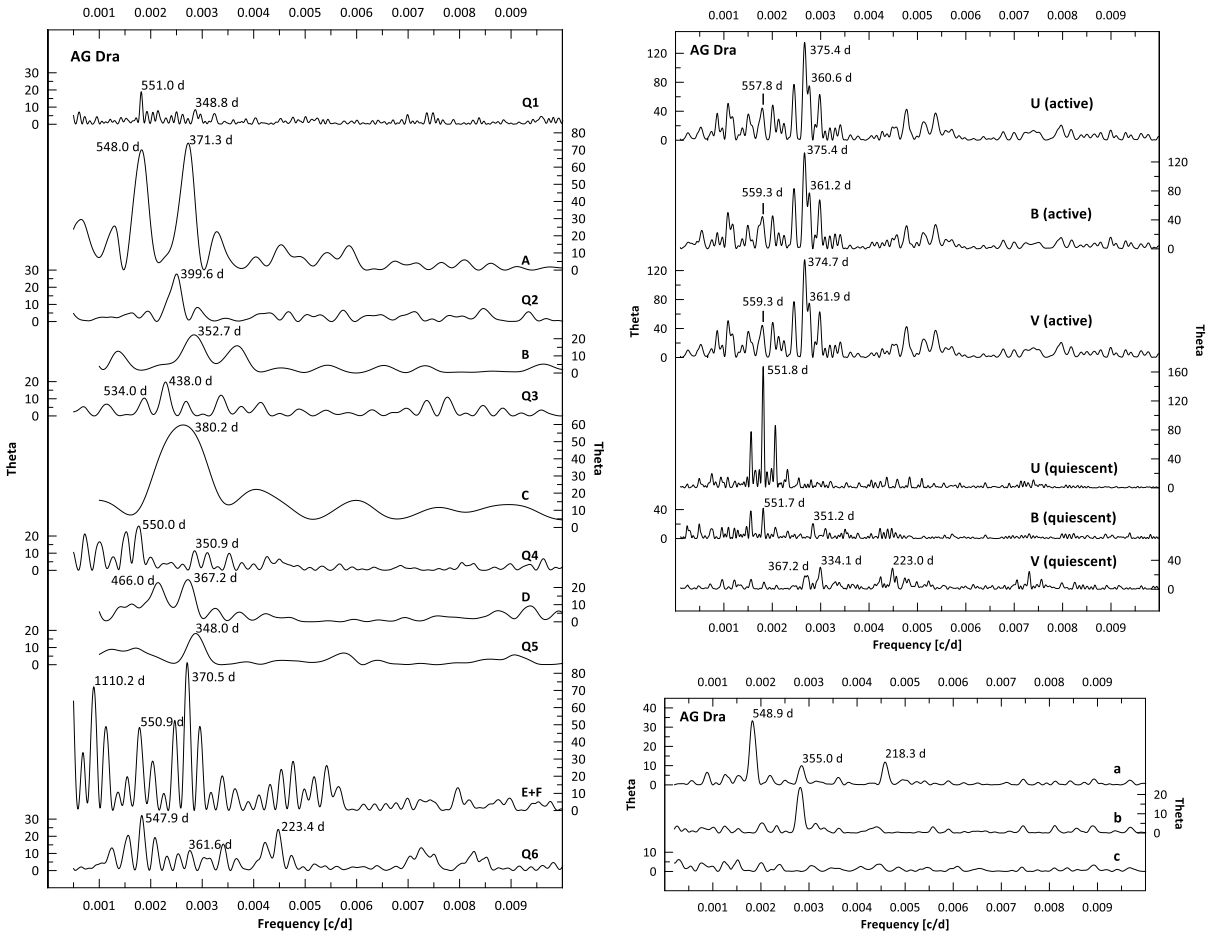

Figure 2: *Left panel*: power spectra of AG Dra taken from historical photographic, photoelectric and CCD data in the *B* filter for particular stages of quiescence (Q1 - Q6) and activity (A - F). *Upper right panel*: power spectra of AG Dra taken from photoelectric and CCD data in *U*, *B* and *V* filters for active (D, E+F) and quiescent (Q4 - Q6) stages. Power spectra for active stages were obtained after removing long-term periods around 1500 and 5400 d, which are related to the global morphology of these active stages. *Lower right panel*: power spectra of AG Dra taken from combined radial velocities based on absorption-line measurements: (a) original data and (b) data with orbital response removed, as well as (c) data with both orbital and probable pulsation response removed. Significant periods are marked with their values.

The light curve after 1966

The first photoelectric photometry of AG Dra was obtained by Belyakina (1969). Since 1974, the system has been observed systematically, mainly photoelectrically in *UBV*. The historical LC of AG Dra over the period 1966 – 2012 was constructed using our compilation of photoelectric and CCD observations in *U*, *B* and *V* filters (Fig. 3). During this period the AG Dra system underwent two (or three?) phases of activity: the first one between the years 1980 and 1986 (D) and the second one between 1993 and 2008 (E+F), with 17 outbursts in total. It is obvious from the LCs (Fig. 3) that the amplitudes of the outbursts increase towards shorter wavelengths, from ∼1 mag in V to ∼3 mag in *U*.

Our statistical analysis shows that the LCs in *U*, *B* and *V* filters were very well correlated (correlation coefficients ∼ 0.9) during the active stages (D, E and F). During the quiescent stages (Q4 – Q6), the correlation coefficients of the LCs in bands *U* and *B* as well as one of the LCs in bands *U* and *V* are less than 0.5, while the variations in the *B* and *V* bands are correlated quite well. This result showed that brightness variations during the quiescent stages of AG Dra in the various bands were caused by different physical mechanisms.

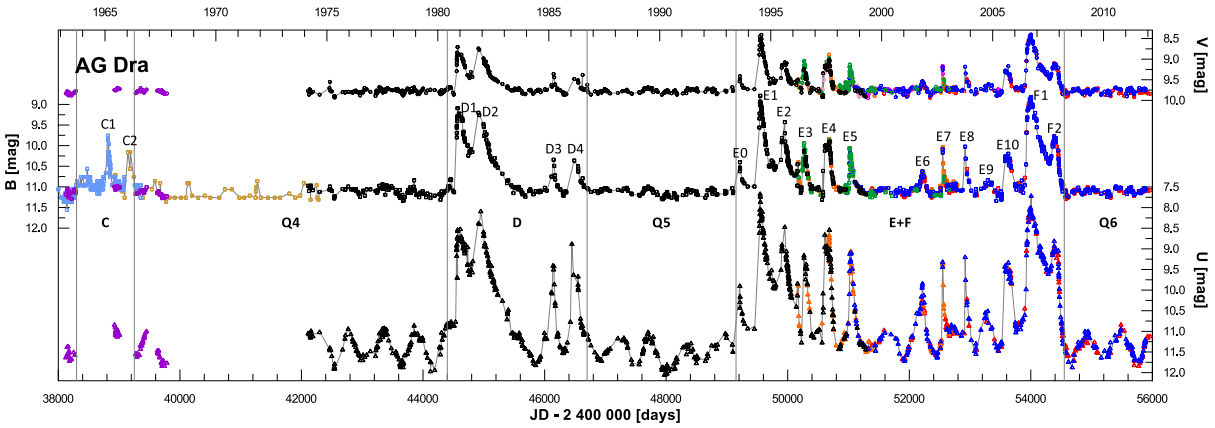

Figure 3: *UBV* LCs from the period 1963–2012 with marked active stages (C, D, E and F) and quiescent ones (Q4, Q5 and Q6). Particular outbursts are assigned as C1–C2, D1–D5, E0–E10 and F1, F2. The thin curves show spline fits to the data points.

The results of period analysis of LCs in *U*, *B* and *V* filters are presented in Table 1 and the corresponding power spectra are depicted in Fig. 2 (upper right panel). The LC in the *U* filter during the quiescent stages is clearly dominated by variations with orbital period ~ 550 d. In the *B* and *V* bands, we found also a shorter period (~ 350 d); however, its value in each quiescent stage changed slightly.

Period analysis of the active stages revealed many significant periods, but most of these periods were more likely related to the complex morphology of the LCs during these stages. The significant period around 370 d is related to the distribution of individual outbursts. The value of this period varies with wavelength and is different for the individual active stages. Statistical analysis shows that the median of the time interval between the individual outbursts is 365 d, while the time intervals vary from 300 to 400 d without an apparent long-term trend.

We can conclude that the results of period analysis of *UBV* LCs unambiguously confirm the presence of the 550-d orbital as well as the 350-d postulated pulsation period.

Table 1. The results of period analysis of particular stages between 1963 and 2012. LCs for each filter were analysed separately. T_{start} is the beginning and T_{end} the end of the given stage. The periods are in order according to their significance.

Phase	T_{start} [MJD]	T_{end} [MJD]	Significant periods [days]		
			***U* filter**	***B* filter**	***V* filter**
Q4	39 250	44 400	551.0 ± 2.4	550.0 ± 10.3; 350.9 ± 4.8	349.6 ± 13.9; 550.0 ± 49.7
D	44 400	46 700	371.9 ± 5.5	367.2 ± 8.1; 466.0 ± 15.2	372.5 ± 6.1
Q5	46 700	49 150	553.6 ± 4.0	348.0 ± 6.7	350.1 ± 7.3
E + F	49 150	54 550	371.2 ± 1.8	370.5 ± 1.9; 1 110.2 ± 18.5[a]; 550.9 ± 9.8	370.5 ± 1.8
Q6	54 550	continue	549.3 ± 2.7	547.9 ± 6.4; 223.4 ± 5.3[b]; 361.6 ± 5.3	357.3 ± 19.8

Notes: [a] The period of 1 110.2 ± 18.5 d is probably only the double of 550.9 ± 9.8 d. [b] The period of 223.4 ± 5.3 d is the one-year alias of 547.9 ± 6.4 d. The global morphology of active stages D and E+F is possibly very well described by the sinusoidal variations with periods around 1 110 d (or double 2 220 d) and 2 500 d (or double 5 000 d).

Period analysis of spectroscopic data

We performed detailed period analysis of radial velocities based on absorption-line measurements with high accuracy (typical errors of 0.4 - 0.8 km s^{-1}) to confirm the presence of periods longer than 1000 d. We detected only two significant periods, 550.4 ± 1.4 and 355.0 ± 1.6 d, related to the orbital motion and cool-component pulsations, respectively. The corresponding power spectra are depicted in Fig. 2 (lower right panel). We can confirm that the data did not contain variability with longer periods.

Outburst mechanisms

Periodical outbursts and their relation to the periodicities in this binary system have been a matter of long-term debate. Recently, the properties of AG Dra have been studied by Formiggini & Leibowitz (2012). The result of their LC period analysis is the detection of the period 373.5 d (the mean time interval between outbursts). Authors interpreted this period as the synodic rotational period of the cool giant with respect to the white dwarf. To secure such a synodic rotational period in a binary with orbital period around 550 d, the giant should rotate in retrograde fashion with a period of 1160 d.

We could not confirm the presence of the period of 1160 d in photometric as well as spectroscopic data. Moreover, such a value of the rotational period of the giant is not typical in symbiotic systems (e.g. table 2 of Formiggini & Leibowitz 2012). The explanation for the retrograde rotation of a component in such an open system from an evolutionary point of view is unclear.

Formiggini & Leibowitz (2012) suggest that the cool giant of AG Dra has a very strong magnetic field, the axis of which is substantially (around 90 degrees) inclined relative to the rotational axis. When the region of the magnetic poles of the giant reaches the tidal bulge, the balance is disrupted and hydrogen-rich matter is thrown into the Roche lobe of the white dwarf. This will release large amounts of gravitational energy, which becomes apparent as an outburst observed in the optical.

According to the opinion of specialists studying stellar magnetic activity across the Hertzsprung–Russell diagram, such very strong magnetic fields of cool giants are not known (Korhonen 2013). The process of balance-breaking by a tidal bulge is unphysical, in view of the fact that the whole surface of the tidally deformed giant in a binary lies on the same equipotential surface.

Formiggini & Leibowitz (2012) explain the alternating active and quiescent stages of AG Dra by the mechanism similar to the solar dynamo (responsible for the solar cycle activity), which takes place in the outer layers of the extensive giant atmosphere. Our analysis of all 124 years brightness history has shown that active stages have recurrence 12 - 16 years, which is in good agreement with the idea of solar-like activity. However, there is no direct evidence of the presence of a reasonably strong magnetic field in the red giants in these systems.

One of the promising explanations of at least some individual outbursts of AG Dra might be the combination nova model proposed for Z And by Sokoloski et al. (2006). In this model, when accretion rate onto the white dwarf exceeds some critical value, thermonuclear reactions are ignited and luminosity of the hot component increases significantly. One of the next tasks would be to study whether the outbursts of AG Dra will fit into such a picture.

Conclusion

We carried out the complex and detailed period analysis of photometric and spectroscopic data of AG Dra. The photometry covers a time interval of 124 years, while the last 39 years of photometric observations are based on systematic photoelectric and CCD monitoring. Spectroscopic data were obtained from absorption line measurements. The results of period analysis of all these data are two real periods present in this symbiotic system: 550 and 350 d, related to the orbital motion and postulated pulsation of the cool component, respectively.

The orbital period is mainly manifested during the quiescent stages at shorter wavelengths (*U* filter), while the pulsation period is present during quiescent as well as active stages at longer wavelengths (*B* and *V* filters). The period analysis of active stages confirmed the presence of a period of around 365 d, which is the median of the time interval between outbursts. It is worth noting that these time intervals vary from 300 - 400 d without an apparent long-term trend. Our detailed analysis shows that most of the longer periods (e.g. 1 330, 1 580, 2 350, 5 500 d) are more likely related to the complex morphology of the LCs during active stages than to the real variability present in this symbiotic system.

The physical mechanism responsible for semi-periodical outbursts as well as recurrence of active stages is not clear. Similarly, the nature of ~ 350 d period which is manifested in photometric as well as spectroscopic data is not fully understood. If these variations are caused by pulsation of the cool component, which physical processes are responsible for such unusual enhancement? Understanding the nature and the physical mechanism of this variability is crucial in order to explain the outburst activity of AG Dra and other classical symbiotic stars. We

suggest that a careful analysis of the light curves together with spectroscopic data as well as comparison of observations in the wide wavelength range from X-rays to radio, would give us first clues in this task. We will present a detailed analysis of the spectroscopic data of AG Dra in our forthcoming paper.

Acknowledgement

This study was supported by the Slovak Academy of Sciences VEGA Grant No. 2/0038/13, by the Slovak Research and Development Agency project APVV-0158-11 and by the realisation of the Project ITMS No. 26220120029.

References

Belyakina T. S., 1969, Izv. Krymskoj Astrofiz. Obs., 40, 39

Formiggini L., Leibowitz E. M., 2012, MNRAS, 422, 2648

Friedjung M., Gális R., Hric L., Petrík K., 2003, A&A, 400, 595

Gális R., Hric L., Friedjung M., Petrík K., 1999, A&A, 348, 533

Garcia, M. R., 1986, AJ, 91, 1400

Korhonen H., 2013, private communication

Meinunger L., 1979, Inf. Bull. Variable Stars, 1611, 1

Mikolajewska J., Kenyon S. J., Mikolajewski M., Garcia M. R., Polidan R. S., 1995, AJ, 109, 1289

Robinson L., 1969, Peremennye Zvezdy, 16, 507

Schwarzenberg-Czerny, A., 1991, MNRAS, 253, 198

Smith V. V., Cunha K., Jorissen A., Boffin H. M. J., 1996, A&A, 315, 179

Sokoloski, J. L., Kenyon, S. J., Espey, B. R., 2006, ApJ, 636, 1002

Zamanov, R. K., Bode, M. F., Melo, C. H. F., Bachev, R., Gomboc, A., Porter, J., Pritchard, J., 2007, MNRAS, 380, 1053

OPEN EUROPEAN JOURNAL ON VARIABLE STARS
September 2014 http://var.astro.cz/oejv ISSN 1801-5964

Blazhko effect at the time of *Kepler*

M.SKARKA [1,2]

(1) Department of Theoretical Physic and Astrophysics, Faculty of Science, Masaryk University, Kotlářská 2, 611 37 Brno Czech Republic, maska@physics.muni.cz
(2) Variable Star and Exoplanet Section of Czech Astronomical Society, Vsetínská 941/78, 757 01 Valašské Meziříčí, Czech Republic

Abstract: I focus on the comparison of the knowledge of the enigmatic Blazhko phenomenon before and after space missions CoRoT and *Kepler*. These two telescopes opened the secret doors of the true diversity of the modulation of RR Lyrae stars. Among many interesting discoveries it was found that higher order multiplets are common characteristics of the frequency spectra of light curves of modulated stars, not unique behaviour of a few objects. This finding resulted in a new mathematical description of modulation which applies methods known from information transfer. Signs of higher radial modes and non-radial modes were detected only due to unprecedented precision of space observations. One of the most important discoveries of the *Kepler* satellite was the uncovering of the alternation of the height of maxima of light changes in modulated stars, the so called period doubling. Based on this new discovery models for explanation of the Blazhko effect were proposed. In addition, Kepler observations clearly showed that Blazhko effect can be irregular in many ways. Therefore, space missions have a major impact on understanding of the Blazhko effect.

Abstrakt: Soustředím se na srovnání znalostí o záhadném Blažkově jevu před a po vypuštění družic CoRoT a *Kepler*. Tyto dva dalekohledy otevřely tajemné dveře pravé diverzity modulace hvězd typu RR Lyrae. Kromě mnoha zajímavých objevů bylo také zjištěno, že multiplety vyšších řádů ve frekvenčních spektrech křivek modulovaných hvězd se vyskytují běžně a ne pouze u několika málo hvězd. Toto zjištění vyústilo v nový matematický popis modulací, který využívá metody známé z teorie přenosu informací. Díky úžasné přesnosti měření vesmírných dalekohledů byly objeveny známky vyšších radiálních a neradiálních módů pulzací. Jedním z nejdůležitějších objevů satelitu *Kepler* bylo odhalení alternace výšky maxim světelných změn křivek modulovaných hvězd, tzv. period doubling. Na základě tohoto objevu byly vytvořeny nové modely pro vysvětlení Blažkova jevu. Navíc se ukázalo, že Blažkův jev může vykazovat různé nepravidelnosti. Vesmírné mise tedy mají zásadní vliv pro pochopení Blažkova jevu.

Many papers dedicated to the Blazhko phenomenon (Blažko, 1907) start with the statement that even one century after its discovery we still do not have proper explanation of this effect. And still this is valid. However, space missions make scientists optimistic, and it seems that we are close to the final solution. But, not so close as we wish. There are still many unanswered questions mainly concerned with the connection between physical parameters and evolutionary effects and modulation of RR Lyrae stars. Also a very recent effort to apply the chaotic behaviour on the *Kepler* data of Blazhko star V783 Cyg failed due to limited time extension, sparse data sampling and some instrumental problems with detrending and data stitching (Plachy et al., 2014). Thus there is still much to do.

The Blazhko effect manifests itself as the quazi-periodic change of the light curve shape. Due to the limited precision of ground based observations it was possible to detect only modulation with relatively high amplitudes both in amplitude and phase variations. However, some precise observations indicate that the modulation can be very weak, even below one tenth of a magnitude (RR Gem and DM Cyg, Jurcsik et al., 2005, Jurcsik et al., 2009a). Space missions revealed that modulation can be even smaller, in the order of only a few hundredths of a magnitude (Kolenberg et al., 2010; Benkö et al., 2010; Benkö et al., 2014).

Almost the entire 20th century the frequency spectra of modulated stars were considered to show only one or maximally two side peaks related to the modulation placed near the basic pulsation frequency and its harmonic. Naturally, it was the result of limited ground-based observations. At the very beginning of the new millennium precise ground-based observations revealed that more side peaks can be detected (MW Lyr and RV UMa, Jurcsik et al. 2008, Hurta et al. 2008). This, in fact, was the end of the models which involved rotation and low order non-radial modes (Dziembowski&Mizerski, 2004; Shibahashi, 2000), because they were not able to explain higher order multiplets than triplets and quintuplets. In CoRoT data of V1127 Aql side peaks which formed multiplets of the eight orders were identified (Chadid et al. 2010). Such high order patterns were found to be common characteristic of frequency spectra of light curves of modulated stars observed by space telescopes.

However, not only higher order frequency patterns, but also multiplets with different spacing between their sidepeaks were detected. Such combination of multiplets is a result of parallel modulations with different frequencies. Just from the beginning of the analysis of *Kepler* data it was obvious that combined modulation is rather common than rare (Benkö et al., 2010; Benkö et al., 2014). Only a few examples were known to show

parallel modulation before space missions (e.g. RS Boo and XZ Cyg, Kanyo, 1980, La Cluyzé et al. 2004). Sodor et al. (2011) found that CZ Lac shows compound modulation with the ratio of modulation frequencies in the ratio of small integer numbers. Three years later, Benkö et al. (2014) showed that about 80 % of all Blazhko stars in *Kepler* field of view show parallel modulation and that the majority of them have modulation frequency ratios in resonance with small integers. In addition, from the shape of the light curves it became evident that many modulated RR Lyrae stars have non-sinusoidal modulation. All these findings and details in the observed Fourier amplitude transforms led to a definition of a new mathematical description of the modulation which involves techniques used in information transfer theory (Benkö, Szabó & Paparó, 2011).

All these discoveries are very interesting. However, we are still not at the end of their list. The first overall study of *Kepler* data (Szabó et al., 2010; Benkö et al., 2010) revealed the alternation of the height of maxima of many of modulated stars (period doubling). This phenomenon results in frequency peaks in the middle of the basic modulation peaks, i.e. at $kf_0/2$, where $k=1,2,3...$ (Fig.1). Such behaviour was not observed in ordinary RR Lyraes. On the other hand it was predicted and observed in cepheids and BL Her stars (Moskalik&Buchler, 1990; Smolec&Moskalik, 2014). Szabó et al. (2010) attributed period doubling to the resonance between the fundamental and the ninth radial overtone in resonance 9:2. This was later confirmed through hydrodynamical modeling and using amplitude formalism (Kolláth et al., 2011, Buchler&Kolláth, 2011). In addition, these authors showed that period doubling can lead to light curve modulation.

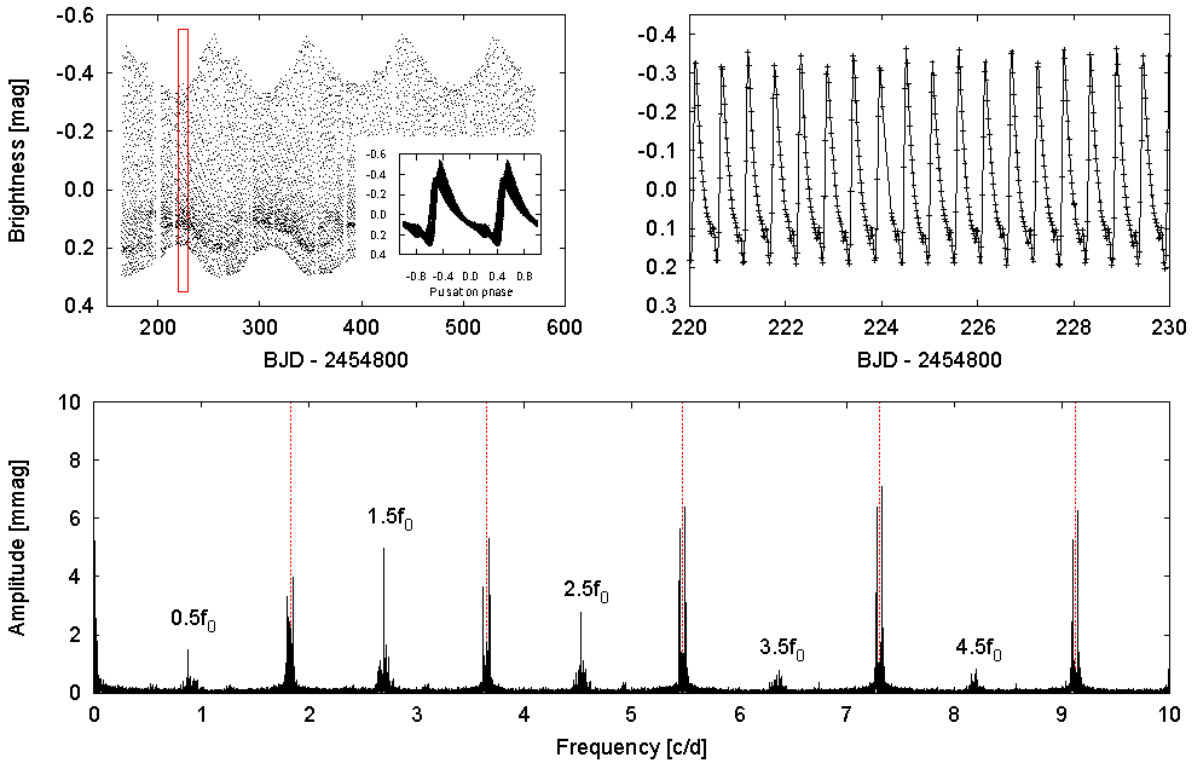

Figure 1: Rectified *Kepler* data of V808 Cyg (according to Benkö et al., 2014). In the top left panel the time series are plotted. The insert shows the data phased with the main pulsation frequency. The region limited by the red rectangle is shown in the top right panel in close up. The alternation of maximum heights is easily seen. Frequency amplitude spectrum after prewhitening with the main pulsation components (depicted by the dotted lines) and the sidepeaks $kf_0 \pm f_m$ is shown in the bottom panel. Except for other modulation sidepeaks, half integer frequencies caused by the period doubling are the most conspicuous.

Although it seems that period doubling could represent the final solution of the Blazhko effect, the situation is not so simple. Firstly, the question why the period doubling was not observed in all modulated stars is unclear. Another bias is that in proposed resonance 9:2 the highest half-integer frequency should be the one at $9/2f_0$, while the highest peak is usually observed at $3/2f_0$.The first attempts for a dynamical analysis of the Blazhko effect applied on *Kepler* data of V783 Cyg showed that even four-year quazi-continual measurements are insufficient for reliable application of models involving nonlinear coupling of pulsation modes (Plachy et al., 2014).

Kepler observations inspired Bryant (2014a) for proposition of another explanation of modulation. He assumed interaction between the sinusoidal fundamental mode and the first radial overtone, which is highly non-sinusoidal with the same frequency as the fundamental mode. In addition, he proposed an extension to his first model when he added an interaction between three modes, and also possibly non-radial modes (Bryant, 2014b). With these models Bryant was able to model light changes of the prototype RR Lyrae star fairly well.

Benkö et al. (2014) analysed the whole available data sets for modulated RRab stars from the *Kepler* field of view. They found that they often show additional radial pulsation modes (first and second overtones). First mode pulsators (RRc stars) were also found to show additional pulsation modes with strange 1.59-1.63 period ratios to the basic pulsation frequency (Moskalik et al. 2013).

Several thousand cycles of RR Lyrae itself allowed a fine analysis of period behavior of this star (Stellingwerf et al., 2013). *Kepler* observations had a major impact also on the estimation of incidence rate of modulated stars among RRab Lyrae type stars, because they allowed the identification of modulation down to milimag level. The current percentage of modulated stars is assumed to be more than 40 % (Jurcsik et al. 2009b; Benkö et al. 2014) with high certainty.

These were only a few of the highlights from the *Kepler* telescope, which were made on RR Lyrae stars. It should be evident that space measurements are of high importance and of unprecedented efficiency.

Acknowledgement

The work has been financed by MU grant MUNI/A/0773/2013.

References

Benkö, J.M., Kolenberg, K., Szabó, R., et al. 2010, MNRAS, 409, 1585

Benkö, J.M., Szabó, R., & Paparó, M. 2011, MNRAS, 417, 974

Benkö, J.M., Plachy, E., Szabó, R., Molnár, L., & Kolláth, Z. 2014, arXiv:1406.5864

Blažko, S. 1907, Astronomische Nachrichten, 175, 325

Bryant, P.H. 2014, ApJL, 783, L15

Bryant, P.H. 2014, arXiv:1408.0263

Buchler, J.R., & Kolláth, Z. 2011, ApJ, 731, 24

Chadid, M., Benkö, J.~M., Szabó, R., et al. 2010, A&A, 510, A39

Dziembowski, W.~A., & Mizerski, T. 2004, AcA, 54, 363

Hurta Zs. et al., 2008, AJ, 135, 957

Jurcsik, J., Sódor, Á., Váradi, M., et al. 2005, A&A, 430, 1049

Jurcsik, J., Sódor, Á., Hurta, Z., et al. 2008, MNRAS, 391, 164

Jurcsik, J., Hurta, Z., Sódor, Á., et al. 2009a, MNRAS, 397, 350

Jurcsik, J., Sódor, Á., Szeidl, B. et al. 2009b, MNRAS, 400, 1006

Kanyo, S. 1980, Information Bulletin on Variable Stars, 1832, 1

Kolenberg K. et al., 2010, ApJ, 713, L198

Kolláth, Z., Molnár, L., Szabó, R. 2011, MNRAS, 414, 1111

LaCluyzé A. et al., 2004, AJ, 127, 1653

Moskalik, P., & Buchler, J.~R. 1990, ApJ, 355, 590

Moskalik, P., Smolec, R., Kolenberg, K., et al. 2013, in: J.C. Suárez, R. Garrido, L.A. Balona, & J. Christensen-Dalsgaard (eds.), *Stellar Pulsations: Impact of New instrumentation and New Insights*, Astrophysics and Space Sci. Proc., Vol. 31 (Berlin, heidelberg: Springer-Verlag), Poster No. 34, arXiv:1208.4251

Plachy, E., Benkö, J.M., Kolláth, Z., Molnár, L., & Szabó, R. 2014, arXiv:1409.4706

Shibahashi, H. 2000, IAU Colloq.~176: The Impact of Large-Scale Surveys on Pulsating Star Research, 203, 299

Sódor, Á., Jurcsik, J., Szeidl, B., et al. 2011, MNRAS, 411, 1585

Smolec, R., Moskalik, P., 2014, MNRAS, 441, 101

Stellingwerf, R.F., Nemec, J.M., & Moskalik, P. 2013, The Kepler RR Lyrae SC data set: Period variation and Blazhko effect, in proceedings to 40 Years of Variable Stars: A celebration of contributions by Horace A. Smith, online book, arXiv:1310.0543

OPEN EUROPEAN JOURNAL ON VARIABLE STARS
September 2014 http://var.astro.cz/oejv ISSN 1801-5964

Flares in eclipsing binary GJ 3236 Cas

L. ŠMELCER [1]

(1) Observatory Valašské Meziříčí, Vsetínská 78, 757 01, Czech Republic, lsmelcer@astrovm.cz

Abstract: In this work we present CCD R-band photometry of GJ 3236 Cas - Algol-type eclipsing binary of spectral class M4. Sudden rapid brightening was observed on March 20, 2014 and April 17, 2014 around secondary minima of the binary. We assume that these events are manifestation of chromospheric and corona activity producing intense flares.

Abstrakt: V této práci je prezentována CCD fotometrie zákrytové dvojhvězdy typu Algol GJ 3236 Cas spektrální třídy M4. 20. března a 17. dubna 2014 bylo pozorováno rychlé zjasnění v blízkosti sekundárních minim. Předpokládá se, že příčinou vzplanutí je aktivita v oblasti chromosféry a korony.

GJ 3236 (*GSC4327 640, R.A.= 03^{h}37^{m}14^s.08 DEC.= +69°10'49".7 Equinox: 2000.0*)

(eclipsing binary type Algol, period 0.77126 day, amplitude 14.27 – 14.50 mag.)

Introduction

Red dwarfs of spectral class M with mass less than 0.6 solar masses are the most abundant group of stars in our galaxy. To date is known only about twenty eclipsing binaries, where both components are red dwarfs, because this low luminosity systems are quite difficult to uncover. Using high dispersion spectroscopy it is possible to determine basic parameters of the components with an accuracy of about 1%. This is sufficient for evolutional modeling of these stars, which also play a key role in our understanding of stellar physics of main sequence stars at the bottom part of the HR diagram.

Massive convection affects the significant part of the atmosphere of red dwarfs and generates a strong magnetic field, source of the high activity, which manifests itself due intensive flares probably originating in the chromosphere and the corona of red dwarfs.

GJ 3236 Cas

Star GJ 3236 Cas was for the first time mentioned in the Third Catalogue of Nearby Stars - Gliese (Gliese, W. 1991). In 1995, Hawley, S.L., et al. published spectroscopic survey of M class dwarfs in the northern hemisphere. In 1999 Hunsche, M. et al. included GJ 3236 Cas in the catalog of nearby stars observed by satellite ROSAT and since then is this object listed also as X-ray source. Gershberg, R. E. et al. in 1999 issued Catalogue of UV Cet-type flaring stars in the solar neighborhood, where GJ 3236 Cas is also shown.

In January 2008, long-term photometric data obtained during Mearth observing campaign (whose main goal was to discover transiting super-Earths around M class dwarfs) revealed GJ 3236 Cas as an eclipsing binary. Irwin et al. published in this paper the basic parameters of both stars: orbital period is 0.77126 days (first observed minimum HJD = 2454734.9959); mass of primary component was determined as 0.376 ± 0.017 Msl (secondary 0.281 ± 0.015 Msl), radius of the primary as 0.3828 ± 0.0072 Rsl (secondary Rsl 0.2992 ± 0.0075) and temperatures T_1 = 3280 K and T_2 = 3205 K. Also based on spectroscopic data the synchronous rotation of both stars with an orbital period was derived.

Instruments, observations and methodology

Presented observations have been obtained on Observatory Valašské Meziříčí using a 254 mm f/4.7 Newtonian reflecting telescope and G2–402 CCD camera (Moravian Instruments) with KAF-0402ME sensor (768x512 pixels, square pixel linear dimension 9 μm). All of the frames have been taken with photometric Johnson-Cousins R-band filter. Exposure time was 60s.

GJ 3236 Cas was observed during 20 nights from March 12, 2014 to May 12, 2014. Between March 12 and April 17 the star was observed 76 hours of total time and this time span represents about 8.7% the interval. During this period – on March 20 and April 17 – two intense brightening were recorded.

Data were analyzed as follows: all frames have been reduced in software package C-Munipack – dark frame calibrated and flat-field corrected. Differential aperture photometry has been performed also in C-Munipack. Comparison stars are UNA 1575-01755929 (comp), UNA 1575-01754797 (chk1) and UNA 1575-01755833 (chk2).

Optical flares

From the recent observations the best documented dwarf eclipsing binary with optical outbursts are CU Cnc and CM Dra. S. B. Qian (2012) reported CCD R-band photometry of CU Cnc flare on October 28, 2009 using the 60-cm telescope on Yennan Observatory. Brightening had amplitude 0.52 mag, duration 73 minutes and characteristic flare shape – rapid increase in pulse phase followed by a gradual decline. With 90 seconds exposure time maximum increase duration can be estimated to about 12 minutes. It is interesting that this eruption was observed almost at the time of primary minimum, therefore this event was most likely associated with secondary component. Subsequently three other small outbursts were observed with duration of 3 minutes and the average amplitude of 0.046 mag.

As a definition of the flare the following criteria were accepted: event has to take several minutes, has to be covered by more than one point and the peak amplitude should not be less than 0.03 magnitude.

Also star CM Dra is known due its relatively high activity. Photometric monitoring lasting over 155 hours carried out in the years 1996-1997 recorded three eruptions within one month (from August 9, 1997 to September 6, 1997). Nelson and Coton (IBVS 5789 - 2007) recorded 6 eruption during six days in the course of campaign lasting 105 hours, both roughly during four orbital periods and in a relatively narrow range of orbital phase 0.26 to 0.52. This suggests that the flares occurred in one large active region. All flares were observed in R-band, while most of this high-energy events are usually observed in other photometric bands U, B and V. Flares in eclipsing binaries were reported previously (Eggen, 1967, Lacy, 1977, Metcalfe 1996, Kim 1997, Kozhevnikov 2004) with amplitudes in the range from 0.02 to 0.7 magnitudes of frequency 0.05 to 0.02 flare per hour.

Optical brightening GJ3236 Cas

Until now no other observation of the flare for this eclipsing binarie was published, although in M. Irwin et al. (Figure 3, phase curves GJ 3236) are two prominent overshooting points on the light curve, which could be interpreted as decline of flare.

The first brightening was recorded on March 20, 2014 at 22h03m13s UT (JDG = 2,456,737.41890). Lasted approximately 12 minutes with amplitude at least 0.4 magnitude. This event was followed by a smaller one with a maximum brightening time 22h24m59s UT (JDG = 2456737.43401) and amplitude of less than 0.1 mag. The event occurred at the phase 0.31185, i.e. 3h29m before observed secondary minimum.

The second brightening was recorded on April 17, 2014 in 23h17m29m UT (JDG = 2,456,765.47048). It took four minutes with an amplitude at least 0.3 magnitude. Event occurred at the phase of 0.6813, thus 3h21m after observed secondary minimum.

After further data processing we were able to detect modulation of the light curve differing from eclipses and flares. Data were analyzed with Peranso program version 2.5. Amplitude period of 0.7712 day was found, which exactly corresponds to the orbital period. The amplitude of modulation was found to be in range 0.05 magnitude.

We assume that these changes in brightness are most likely connected with large spots on the surface of the star, periodically appearing and disappearing due orbital geometry. Generally, more spots are expected on a warmer primary star, which can modulate the light curve of the system between the eclipses. Since the brightness modulation minima occurs approximately at the binary phase of 0.8, that is, when near side of the primary component relative to the observer is visible, the spots are likely to reside on the primary component. This fact, among others, confirms the previously determined binary system with bound rotation.

Conclusion

In this work we present observational results of flares in dwarf eclipsing binary star GJ 3236 Cas. During March and April 2014 two distinctive flares were recorded. On the phase light curve is apparent modulations with amplitude of 0.05 magnitudes and period equal to the orbital period of the eclipsing binaries. This modulations is most likely due to presence of spots on surface one of the stars. In the following months we plan further monitoring of this star and other similar eclipsing systems.

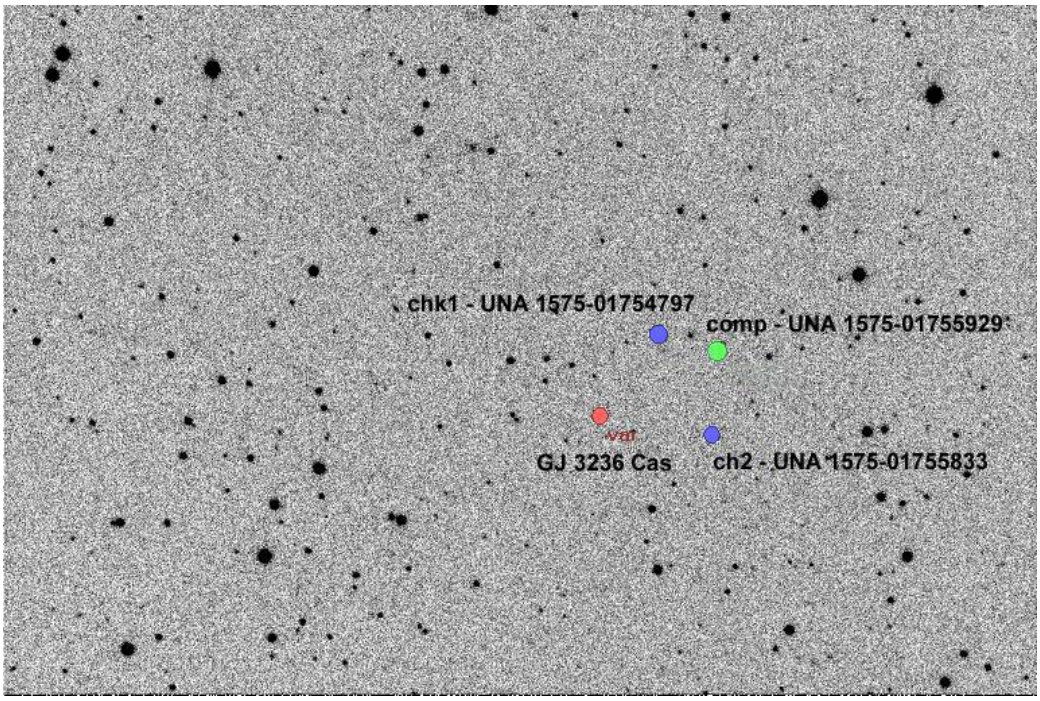

Figure 1: Starfield around GJ 3236 Cas (red dot) with comparison and check stars (green and blue).

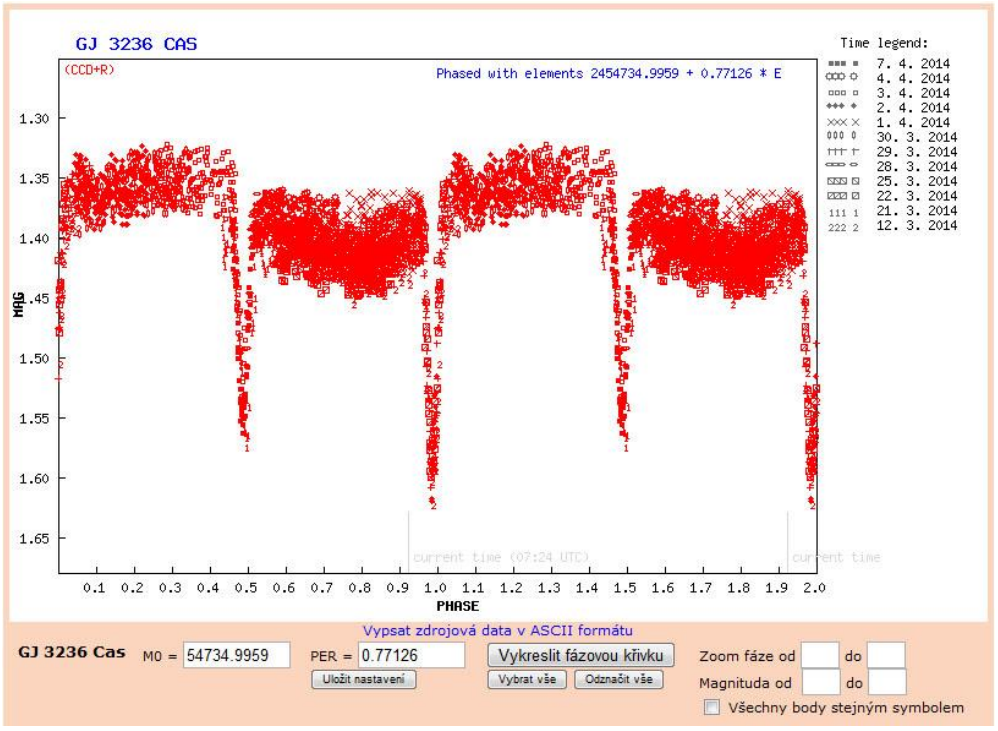

Figure 2: Phase curve showing CCD R-band data obtained from March 12, 2014 to April 7, 2014. Besides primary and secondary minima the modulation of brightness is also visible. Period modulation is equal to orbital period.

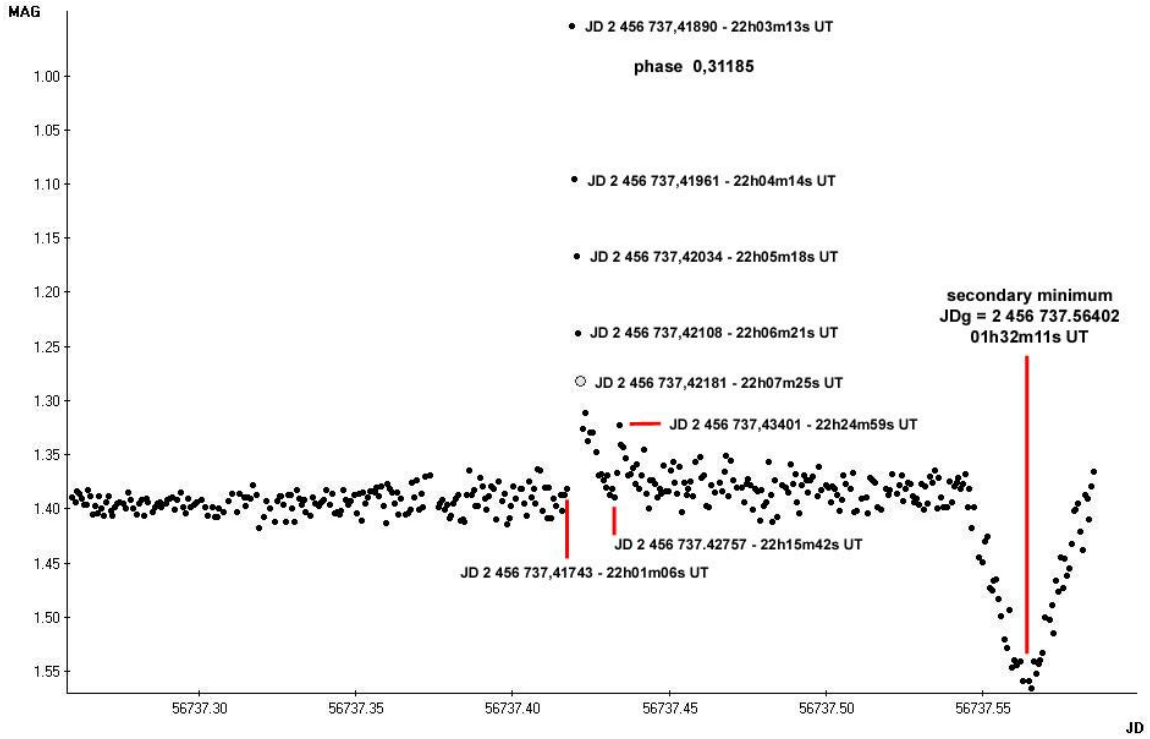

Figure 3: Light curve of GJ3236 Cas eclipsing binary from March 20, 2014 (JD 2456737) with a sudden brightening lasting for 12 minutes. Secondary minimum is following. Data were taken in R-band with a Newtonian telescope (d=254 mm, f/4.7) and G2-CCD camera.

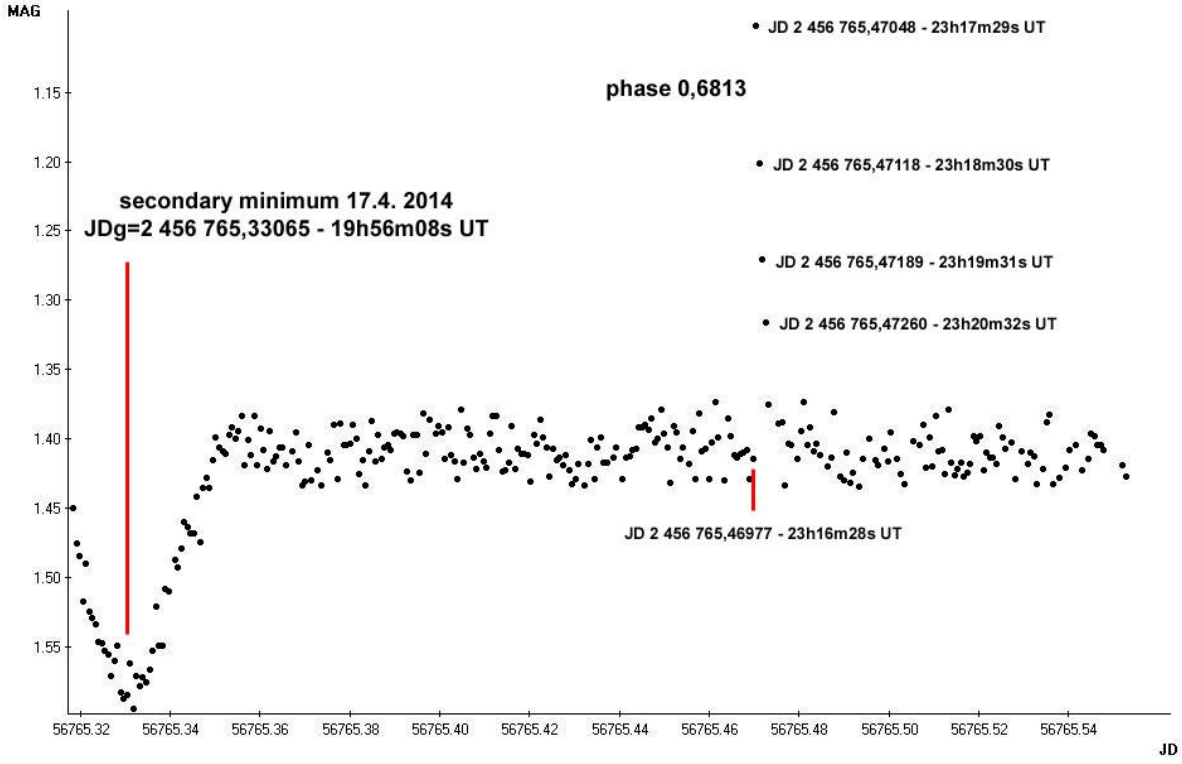

Figure 4: Light curve of GJ3236 Cas eclipsing binary from April 17, 2014 (JD 2 456 765) with a sudden brightening lasting for about 4 minutes. Secondary minimum is preceding. Data were taken in R-band with a Newtonian telescope (d=254 mm, f/4.7) and G2-CCD camera.

References:

Gliese, W., Jahreiss, H., 1991, Preliminary Version of the Third Catalogue of Nearby Stars

Hawley, Suzanne L., Gizis, John E., Reid, I. Neill, 1996, AJ, 112, 2799

Hünsch, M., Schmitt, J. H. M. M., Sterzik, M. F., Voges, W., 1999, A&AS, 135, 319

Gershberg, R. E., Katsova, M. M., Lovkaya, M. N., Terebizh, A. V., Shakhovskaya, N. I., 1999, A&AS, 139, 555

Irwin, J., Charbonneau, D., Berta, Z. K., Quinn, Samuel N., 2009, ApJ, 701, 1436

Motl, D., 2009, C-Munipack, http://c-munipack.sourceforge.net/

Vanmunster T., 2004, PERANSO 2.5, CBABelgium.com

OPEN EUROPEAN JOURNAL ON VARIABLE STARS
September 2014 http://var.astro.cz/oejv ISSN 1801-5964

FRAM telescope – monitoring of atmospheric extinction and variable star photometry

J. JURYŠEK[1,2,1], K. HOŇKOVÁ[2], M. MAŠEK[1,2]

(1) Institute of Physics of the Czech Academy of Sciences, Na Slovance 1999/2, 182 21 Praha 8
(2) Variable Star and Exoplanet Section of Czech Astronomical Society

Abstract: The FRAM (F/(Ph)otometric Robotic Atmospheric Monitor) telescope is a part of the Pierre Auger Observatory (PAO) located near town Malargüe in Argentina. The main task of the FRAM telescope is the continuous night-time monitoring of the atmospheric extinction and its wavelength dependence. The current methodology of the measurement of a atmospheric extinction and for instrumentation properties also allows simultaneous observation of other interesting astronomical targets. The current observations of the FRAM telescope are focused on the photometry of eclipsing binaries, positional refinement of minor bodies of the Solar system and observations of optical counterparts of gamma ray bursts. In this contribution, we briefly describe the main purpose of the FRAM telescope for the PAO and we also present its current astronomical observing program.

Abstrakt: Dalekohled FRAM (F/(Ph)otometric Robotic Atmospheric Monitor) je součástí Observatoře Pierra Augera (PAO) a nachází se blízko města Malargüe v Argentinské pampě. Primárním účelem dalekohledu je měření okamžitých hodnot atmosférické extinkce a její závislosti na vlnové délce. Metodika měření extinkčních koeficientů a technické vlastnosti dalekohledu umožňují současně s měřením atmosférické extinkce pozorovat množství zajímavých astronomických cílů. V současné době je dalekohled využíván k měření kompletních světelných křivek vybraných zákrytových dvojhvězd, ke zpřesňování poloh nově objevených planetek a komet a také k pozorování optických protějšků záblesků záření gama. V tomto příspěvku stručně popisujeme význam dalekohledu FRAM pro PAO a také představujeme aktuální astronomický pozorovací program dalekohledu.

Introduction

The FRAM (F/(Ph)otometric Robotic Atmospheric Monitor) telescope is a part of the Pierre Auger Observatory (PAO) and it was built and operated by Institute of Physics AS CR. The telescope and the PAO are located near town Malargüe (69°W, 35°S, 1400 m a.s.l.) in Mendoza province in Argentina. The PAO is currently the world largest detector of the ultra-high energy cosmic rays (UHECRs). There are two kinds of the cosmic rays detectors – surface detector and fluorescence detector. The surface detector is an array of about 1 600 water Cherenkov stations arranged in a regular triangular grid with the 1.5 km distance between stations, which are deployed over an area of 3000 km^2. Fluorescence detectors are telescopes which are capable of measuring ultraviolet fluorescence light produced during cosmic ray shower development. The total amount of fluorescence light integrated over the whole air shower track is proportional to energy of an incoming primary cosmic ray particle. Thus the atmosphere plays the role of a huge calorimeter which properties should be monitored. There are many devices with the purpose of monitoring the atmospheric conditions in the PAO, including the Czech FRAM telescope (The Pierre Auger Collaboration, 2012)[2].

Instrumentation

Primary part of the FRAM telescope (see Fig. 1) is the 0.3m Meade Schmidt-Cassegrain tube with the CCD camera G2-1600 made by Moravian instruments[3] and with field of view (FOV) of only 16'×24', so we call it Narrow field (NF). Atop the main telescope is attached Nikkor 300 mm lens with CCD G4-16000 with huge FOV 7°×7°, so we call it Wide field (WF). Both cameras are equipped with Johnson-Bessel BVRI photometric filters. Magnitudes of stars for precision color photometry range from about 6 to 9 mag for WF and from about 9 to 13 mag in NF. Telescope works in fully automated mode using Remote Telescope System 2 (RTS2) software package (Kubánek, 2010)[4].

[1] Email: nadseni.promenari@astronomie.cz
[2] For a more detailed description of the PAO, see the project page: http://www.auger.org/
[3] http://www.mii.cz/
[4] http://www.rts2.org

Figure 1: The FRAM telescope.

Monitoring of atmospheric extinction

The main task of the FRAM telescope is the continuous night-time monitoring of the atmospheric integral aerosol optical depth and its wavelength dependence. Atmospheric extinction is measured by photometry of selected non-variable stars. Measured instantaneous instrumental magnitudes are after color calibration compared with catalogue magnitudes. To obtain the aerosol part of extinction/optical depth it is necessary to subtract Rayleigh part of extinction derived from atmospheric models. Wavelength dependence of the resulting aerosol part of the atmospheric extinction can be parameterized by Angström coefficient. The final results of data processing should be continuous night time evolution of Angström coefficient (Prouza et al., 2010). In the left Fig. 2 it is shown typical time dependency of the atmospheric total optical depth, and in the right it is shown time dependency of Angström coefficient for the same night. The FRAM telescope is used not only for the monitoring of atmospheric extinction, but also for the so called Shoot-the-shower (StS) program designed for rapid monitoring of atmospheric conditions along the trajectories of air showers of high interest. For particle physics are especially interesting the showers with anomalous longitudinal profiles. StS is crucial to distinguish the cases, when anomalous profile is real due to special development of cosmic ray shower, or if it is caused by cloud transition or other atmospheric phenomena. For detailed description of StS see Blažek (2014).

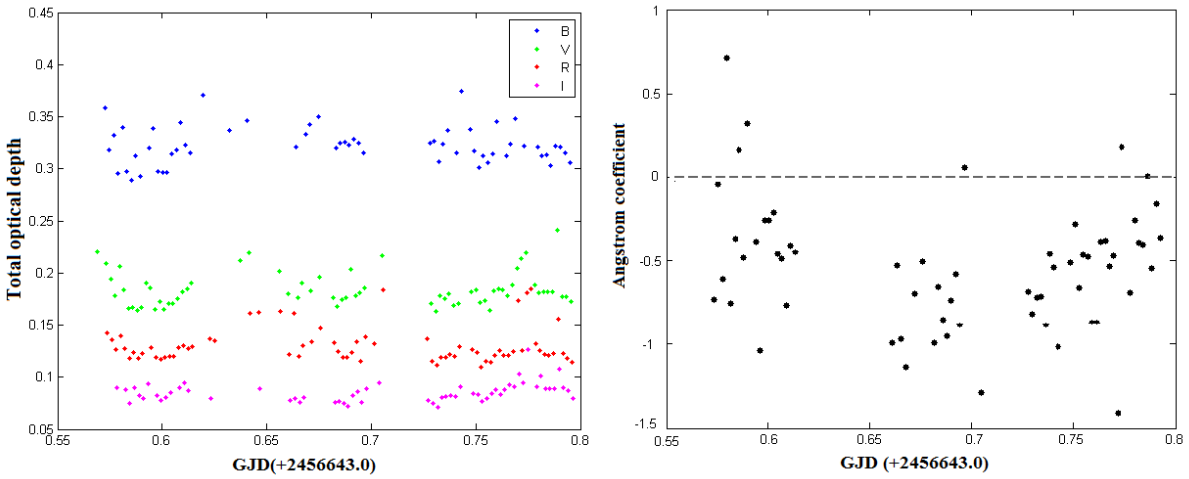

Figure 2: *Left* - Immediate optical thickness of the atmosphere in BVRI during one night. *Right* - The Angström coefficient shows immediate wavelength dependence of atmospheric extinction.

Variable star photometry

There are about 10^2 stars in the FOV of NF and about 10^4 stars in the FOV of WF. Therefore, we can choose stars for extinction measurement appropriately so that the other astronomical objects will be in the same field. Because the FRAM telescope observes every night, following its primary goals, it seems to be most appropriate

to dedicate its other free time to a long time color photometry of variable stars and to completion of phase curves. At present, we focus to observations of interesting eclipsing binaries which show light time effect or apsidal motion. We also focus our attention to eclipsing binaries with insufficiently covered phase curves or with unknown elements. We perform all of our observations based on the recommendations of professional astronomers from Czech Republic and also from abroad. Our cooperation includes Charles University in Prague (CZ), Masaryk University in Brno (CZ), Pulkovo Observatory in Russia and Odessa National Maritime University in Ukraine. All scientific results will be published separately, but a sample of our observations is illustrated and briefly described in the Fig. 3.

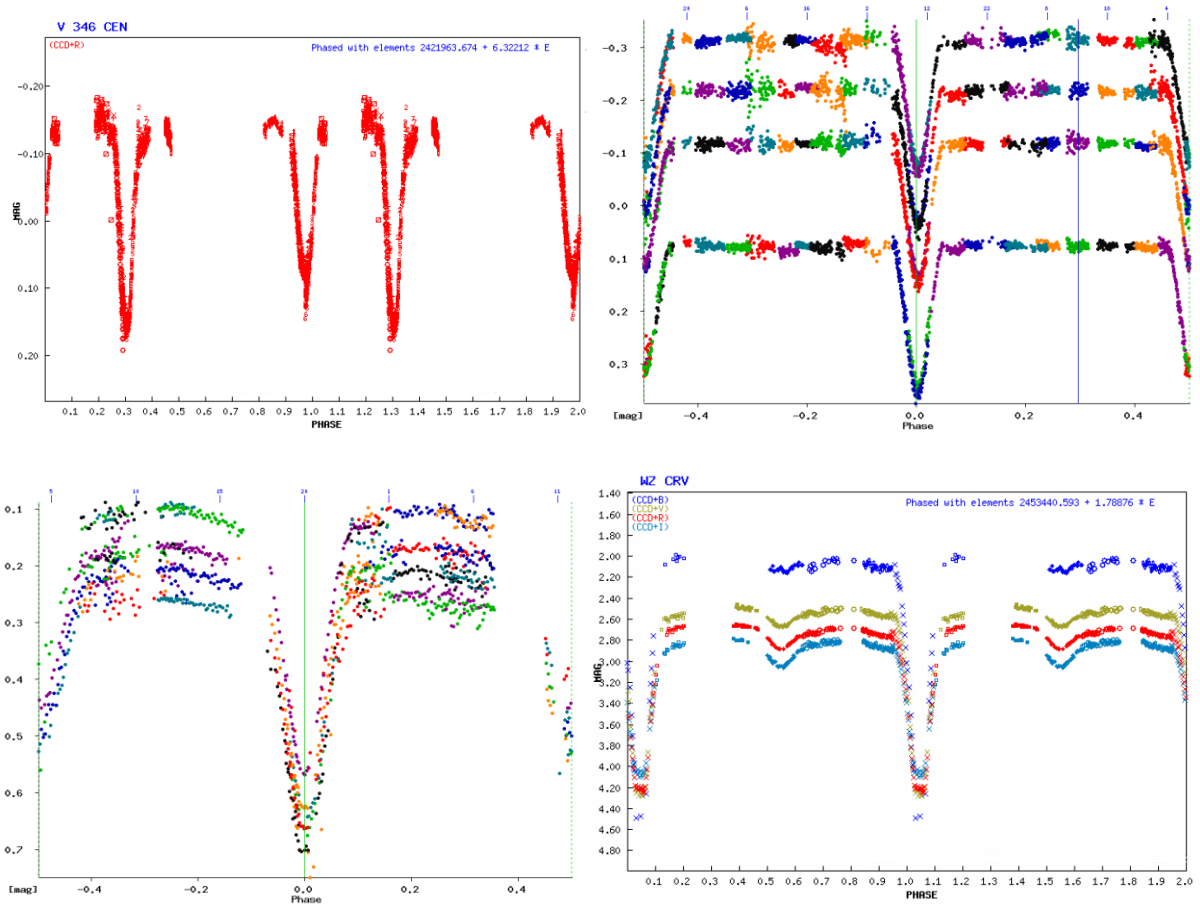

Figure 3: *Upper left* – V 346 Cen, long periodic eccentric eclipsing binary. *Upper right* – V 949 Cen, part of a triple system with 350 years period of the third body. *Lower left* – V1293 Sco, member of NGC 6231 open cluster, which contains 10 poorly described eclipsing binaries. *Lower right* – Yet incomplete phase curve of spotted variable WZ Crv, observed for to the study of spots evolution.

Byproduct of processing of large amounts of data from the FRAM telescope (daily about 4 GB of FITS frames) are many basically random discoveries of new variable stars. Using Muniwin's "find variable" algorithm (Motl, 2010) we have already discovered 25 variable stars, e.g. multiperiodic Delta Scuti CzeV591 Cru (Hoňková et al., 2014a). In the FOVs of NF and WF were also found many previously known eclipsing binaries during eclipses. All timings of these minima were uploaded to B.R.N.O. database[5]. For example, there are 155 minima timings of southern eclipsing binaries from the FRAM telescope in new "B.R.N.O. Contributions #39 Times of minima" publication (Hoňková et al., 2014b, in prep.).

Other targets

In its spare time, the FRAM telescope is also observing other interesting objects in our Solar system (mostly comets and asteroids) and exoplanet transits.

In this category, the FRAM telescope observes mainly recently discovered Near-Earth asteroids and performs confirmation observations and follow-up astrometry of these objects for more precise determination of their trajectories. The location of the FRAM in Argentina is convenient for the observations of neglected comets, which are observable only from the southern hemisphere. With the FRAM telescope three comets:

[5] http://var2.astro.cz/

260P/McNaught (Mašek et al., 2012), 296P/Garradd (Mašek & Williams, 2014) and 300P/Catalina (Mašek et al., 2014) have been recovered.

Conclusions

The aims of this contribution are to present the current observing program of the FRAM telescope and to outline some interesting results, which will be published in separate papers. The current methodology of the atmospheric extinction measurement allows many other astronomical activities like photometry of selected variable stars or astrometry of minor bodies of the Solar system. At present, the FRAM telescope is connected to the global network of robotized telescopes - GLORIA[6]. Though the GLORIA project anyone can take scientific or artistic images of selected astronomical object of their own interest.

Acknowledgements

The operation of the robotic telescope FRAM is supported by the EU grant GLORIA (No. 283783 in FP7-Capacities program) and by the grant of the Ministry of Education of the Czech Republic (MSMT-CR LG13007).

References

Blažek, J., 2014, Master thesis, Charles University, Prague

Kubánek, P., 2010, Advances in Astronomy, 2010

Hoňková, K., Juryšek, J., Mašek, M., Paunzen, E., Zejda, M., 2014, IBVS, 6110, 1

Hoňková et al., 2014b, in prep., OEJV, B.R.N.O. Contributions #39 Times of minima

Mašek, M., Williams, G., V. & Nakano, S., 2012, Central Bureau Electronic Telegrams, 3114, 1

Mašek, M. & Williams, G., V., 2014, Central Bureau Electronic Telegrams, 3774, 1

Mašek, M., Nakano, S. & Williams, G., V., 2014, Central Bureau Electronic Telegrams, 3852, 1

Motl, D., 2010, C-Munipack Project, http://c-munipack.sourceforge.net/

Prouza, M., Jelínek, M., Kubánek, P., et al., 2010, Advances in Astronomy, 2010

The Pierre Auger Collaboration, 2012, Journal of Instrumentation, 7, 9001

[6] http://gloria-project.eu/

OPEN EUROPEAN JOURNAL ON VARIABLE STARS
September 2014 http://var.astro.cz/oejv ISSN 1801-5964

14 New Variable Stars in SvkV Catalogue.

M. VRAŠŤÁK [1,2]

(1) Kľúčiny 74, Liptovská Štiavnica, 034 01, Slovakia, vrastak@post.sk
(2) Variable Star and Exoplanet Section of Czech Astronomical Society

Abstract: I report the discovery of a 14 new variable stars in the Per, Cas, And, Oph, and Cyg constellations. Stars were observed bay the Liptovská Štiavnica observatory on years 2011 – 2014 and were added to the SvkV catalogue. The variable type and the elements of each stars are identified and presented.

Abstrakt: V období od roku 2011 do roku 2014 som vložil do SvkV katalógu celkom 14 nových premenných hviezd, ktoré boli identifikované v súhvezdiach Per, Cas, And, Oph, a Cyg. Premenné hviezdy som pozoroval na svojom observatóriu v Liptovskej Štiavnici. V tomto článku uvádzam typy a svetelné elementy všetkých identifikovaných nových premenných hviezd.

Introduction

Based on the observing of the known variable stars MW Cas, V449 And V2637 Oph, V859 Cyg and exoplanet HAT-P 29b, I have found in the same fields fourteen new variable stars. I followed the variation of this variable over a period of several days. Observations mentioned above were taken at Liptovská Štiavnica Observatory on the Newton telescope 0.24m f/5 reflector and G2-1600 CCD camera. In the case of observing HAT-P 29b and MW Cas all CCD images were taken using a clear filter. In the case of observing V449 And, V2637 Oph and V859 Cyg CCD images were taken using V and Rc filter. CCD frames were mostly reduced by C-MuniPack code (Motl, 2009), the well-known adaptation of MuniPack code (Hroch, 1998), based on DaoPhot routines (Stetson, 1987). All frames were dark-frame and flat-field corrected before application of further reduction steps. Minima timings and errors were determined by online procedure Minima Timing of Eclipsing Binaries (Brát, Mikulášek, Pejcha 2012). The comparison stars were chosen to be in the field of view of telescope. Magnitudes of used comparison stars were taken from TYCHO catalogue. The magnitudes of the newly found variables were calculated using transform coefficients into the standard Johnson photometric system, band V. Used transform coefficients were: Cb = 0.8866, Cv = -0.0617, Cr = -1.1418, Ci = -1.0059. For each star a finding chart is shown, as well as the calculated elements for epoch and period, a phase diagram and an identification of the variable type are given, too. All results were determined using Peranso - light curve and period analysis software.

Variable Star	Name	RA	DEC	Field	Type
SvkV26 Per	GSC 3293 1438	02 11 29.63	+51 32 22.55	HAT-P 29b	EA
SvkV27 Per	USNO B1.0 1414-0059665	02 11 09.24	+51 29 10.91	HAT-P 29b	EW
SvkV29 Per	USNO B1.0 1417-0069121	02 13 00.97	+51 43 02.81	HAT-P 29b	EW
SvkV30 Per	GSC 3293 0988	02 10 59.39	+51 42 52.26	HAT-P 29b	EB
SvkV31 Cas	USNO B1.0 1451-0009950	00 16 41.29	+55 06 52.84	MW Cas	EW
SvkV32 Cas	USNO B1.0 1453-0009166	00 15 39.20	+55 19 30.08	MW Cas	EW
SvkV35 And	TYC 3281-85	02 08 46.33	+46 26 03.07	V449 And	EW
SvkV36 And	GSC 3285 1170	02 09 47.52	+47 04 32.67	V449 And	EB
SvkV37 And	USNO B1.0 1366-0046496	02 10 19.07	+46 40 43.78	V449 And	EB
SvkV38 And	USNO B1.0 1367-0045541	02 10 25.37	+46 45 20.84	V449 And	EW
SvkV41 Oph	USNO B1.0 0954-0288850	17 18 03.43	+05 24 28.00	V2637 Oph	EW
SvkV42 Cyg	USNO B1.0 1189-0356565	19 27 07.75	+28 58 49.54	V859 Cyg	EW
SvkV43 Cas	USNO B1.0 1448-0009592	00 16 18.37	+54 53 58.10	MW Cas	EW
SvkV 44 Cas	USNO B1.0 1450-0010013	00 17 01.59	+55 03 33.28	MW Cas	EB

Table 1: Identifications and positions of the new variables, coordinates taken from GUIDE 9.0 catalogue, epoch 2000.

Variable Star	M0 HJD	P (d)	P(d) err	mag V	mag V err	amplitude
SvkV26 Per	2454363.651	1.80037	± 0.00013	13.569	± 0.078	0.24
SvkV27 Per	2455798.193	0.23646	± 0.00046	14.915	± 0.078	0.47
SvkV29 Per	2455798.122	0.38865	± 0.00042	16.048	± 0.078	0.23
SvkV30 Per	2454332.765	0.98050	± 0.00051	12.447	± 0.078	0.35
SvkV31 Cas	2455830.923	0.29718	± 0.00024	15.275	± 0.031	0.31
SvkV32 Cas	2455827.933	0.47740	± 0.00673	15.601	± 0.031	0.18
SvkV35 And	2456153.227	0.51782	± 0.00023	11.432	± 0.036	0.21
SvkV36 And	2456152.867	0.33766	± 0.00002	13.024	± 0.036	0.35
SvkV37 And	2456153.249	0.38298	± 0.00006	14.209	± 0.036	0.47
SvkV38 And	2456152.420	0.44394	± 0.00004	14.716	± 0.036	0.75
SvkV41 Oph	2456431.410	0.34127	± 0.00186	14.902	± 0.114	0.50
SvkV42 Cyg	2456461.360	0.45050	± 0.00182	15.485	± 0.028	0.30
SvkV43 Cas	2455820.210	0.36642	± 0.00046	16.506	± 0.031	0.34
SvkV44 Cas	2455819.955	0.81994	± 0.00276	14.576	± 0.031	0.17

Table 2: Elements of the new variable stars and observing periods.

Variable Star	Ref. Star	Ref magV	Ref mag err	B-V	B-V err
SvkV26 Per	TYC 3293 1459	11.223	± 0.078	0.107	± 0.075
SvkV27 Per	TYC 3293 1459	11.223	± 0.078	0.107	± 0.075
SvkV29 Per	TYC 3293 1459	11.223	± 0.078	0.107	± 0.075
SvkV30 Per	TYC 3293 1459	11.223	± 0.078	0.107	± 0.075
SvkV31 Cas	TYC 3657 1313	9.928	± 0.031	0.888	± 0.039
SvkV32 Cas	TYC 3657 1313	9.928	± 0.031	0.888	± 0.039
SvkV35 And	TYC 3281 1988	9.877	± 0.036	0.458	± 0.037
SvkV36 And	TYC 3281 1988	9.877	± 0.036	0.458	± 0.037
SvkV37 And	TYC 3281 1988	9.877	± 0.036	0.458	± 0.037
SvkV38 And	TYC 3281 1988	9.877	± 0.036	0.458	± 0.037
SvkV41 Oph	TYC 408 507	11.044	± 0.114	1.479	± 0.227
SvkV42 Cyg	TYC 2137 2923	9.655	± 0.028	0.684	± 0.031
SvkV43 Cas	TYC 3657 1313	9.928	± 0.031	0.888	± 0.039
SvkV44 Cas	TYC 3657 1313	9.928	± 0.031	0.888	± 0.039

Table 3: Used comparison stars, magnitudes taken from TYCHO catalogue.

Observations of SvkV27 Per, SvkV28 Per, SvkV29 Per, SvkV30 Per

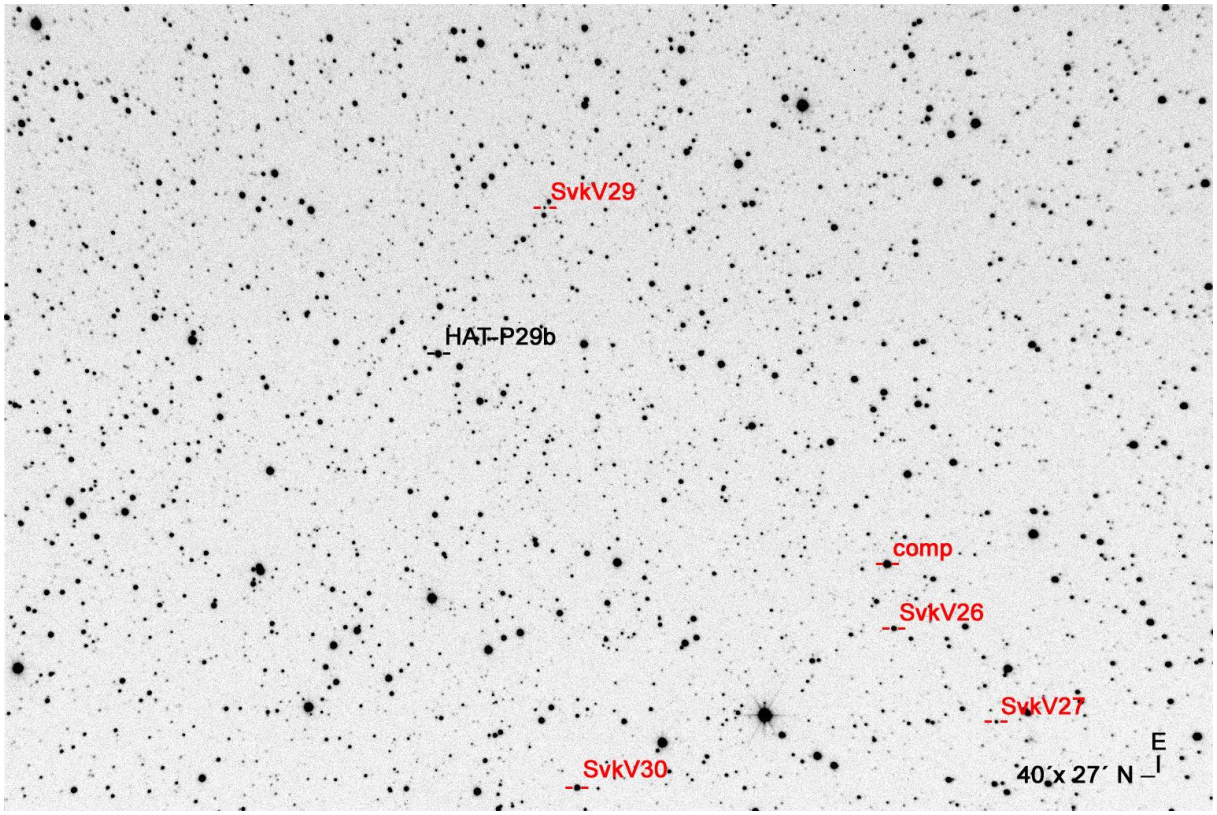

Figure 1: CCD picture of the variable stars SvkV27 Per, SvkV28 Per, SvkV29 Per, SvkV30 Per and the comparison star TYC 3293 1459.

SvkV26 Per (*GSC 3293 1438, R.A.= 0211 29.63s DEC.= +513222.55 Equinox: 2000.0*)
(type EA, period 1.80037 day, brightness 13.57 (V) mag, amplitude 0.24 mag.)

SvkV26 Per	T observed HJD	Error 1σ Bootstrapping	O - C	Minimum	observer
No.	d	±d	d	type	
Min1	2454363.65117	0.00189	0.0001	I	SWASP
Min2	2454419.4619	0.00347	0.0000	I	SWASP
Min3	2455798.54222	0.00052	-0.0006	I	MV

Table 4: SvkV26 Per, Times of minimum are given in HJD. Min1 and Min2 were obtained from SuperWASP public archive.

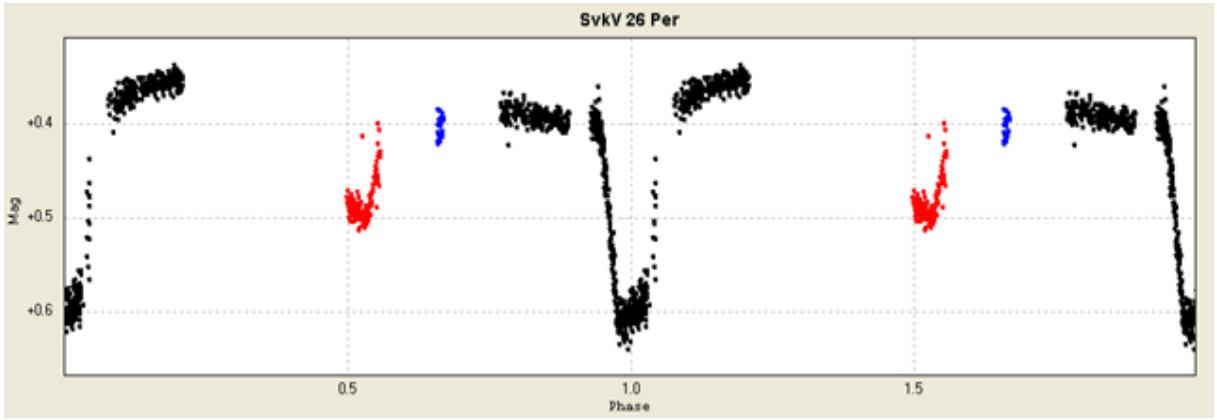

Figure 2: Phase diagram (light curve) for SvkV26 Per, each colour represents another observation set.

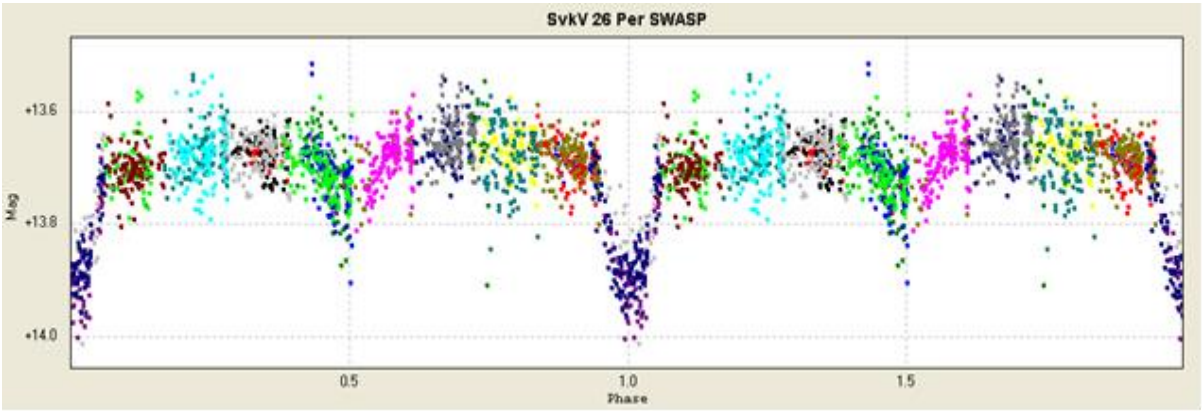

Figure 3: Phase diagram (light curve) for SvkV26 Per, data obtained from SuperWASP public archive.

SvkV27 Per (*USNO B1.0 1414-0059665, R.A.= 021109.24 DEC.= +512910.91 Equinox: 2000.0*) (type EW, period 0.23646 day, brightness 14.92 (V) mag, amplitude 0.47 mag.)

SvkV27 Per	T observed HJD	Error 1σ Bootstrapping	O - C	Minimum	observer
No.	d	±d	d	type	
Min1	2455798.43053	0.00078	0.0009	II	MV
Min2	2455798.54491	0.00032	-0.0030	I	MV
Min3	2455805.40102	0.00023	-0.0042	I	MV
Min4	2455805.52430	0.00024	0.0009	II	MV
Min5	2455811.43690	0.00023	0.0020	II	MV
Min6	2456956.36993	0,00043	0.0005	II	MV

Table 5: SvkV27 Per, Times of minimum are given in HJD.

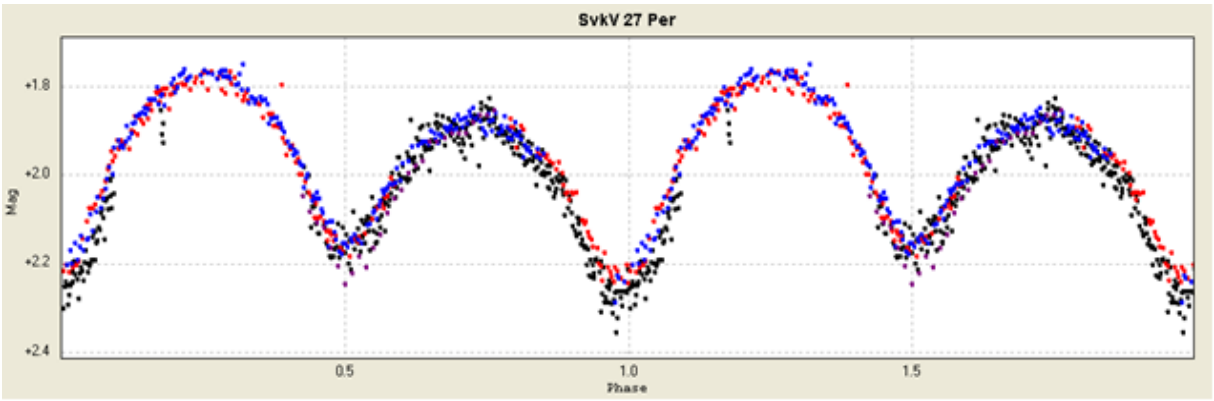

Figure 4: Phase diagram (light curve) for SvkV27 Per, each colour represents another observation set.

SvkV29 Per (*USNO B1.0 1417-0069121, R.A.= 021300.97 DEC.= +514302.81 Equinox: 2000.0*)
(type EW, period 0.38865 day, brightness 16.05 (V) mag, amplitude 0.23 mag.)

SvkV29 Per	T observed HJD	Error 1σ Bootstrapping	O - C	Minimum	observer
No.	d	±d	d	type	
Min1	2455798,50691	0,00164	-0.0037	I	MV
Min2	2455799,48182	0,00127	-0.0005	II	MV
Min3	2455805,51258	0,00144	0.0062	I	MV
Min4	2455811,33440	0,00221	-0.0017	I	MV

Table 6: SvkV29 Per, Times of minimum are given in HJD.

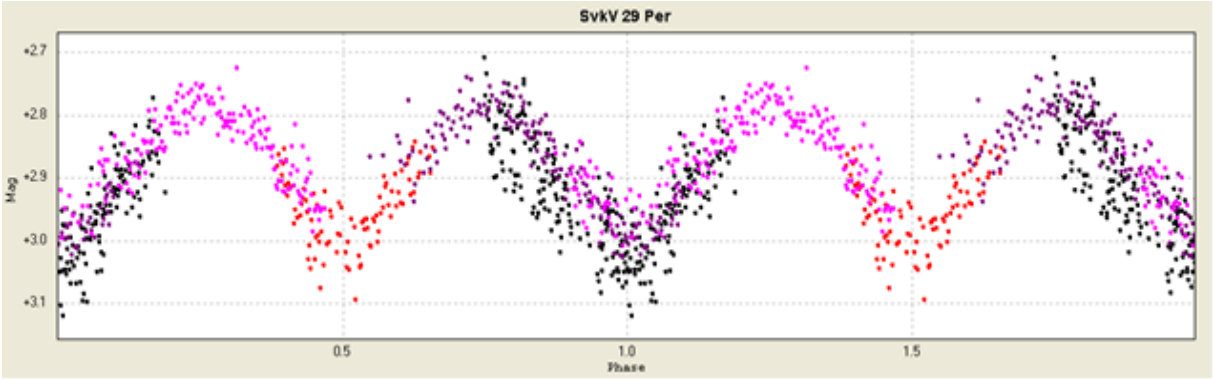

Figure 5: Phase diagram (light curve) for SvkV29 Per, each colour represents another observation set.

SvkV30 Per (*GSC 3293 0988, R.A.= 021059.39 DEC.= +514252.26 Equinox: 2000.0*)
(type EB, period 0.98050 day, brightness 12.45 (V) mag, amplitude 0.35 mag.)

SvkV30 Per	T observed HJD	Error 1σ Bootstrapping	O - C	Minimum	observer
No.	d	±d	d	type	
Min1	2454337.66500	0.00270	-0.0025	I	SWASP
Min2	2454338.64566	0.00221	-0.0023	I	SWASP
Min3	2454361.69511	0.00254	0.0054	II	SWASP
Min4	2454362.67629	0.00211	0.0060	II	SWASP
Min5	2454363.65105	0.00302	0.0003	II	SWASP
Min6	2454387.66465	0.00199	-0.0083	I	SWASP

Table7: SvkV30 Per, Times of minimum are given in HJD. All data obtained from SuperWASP public archive.

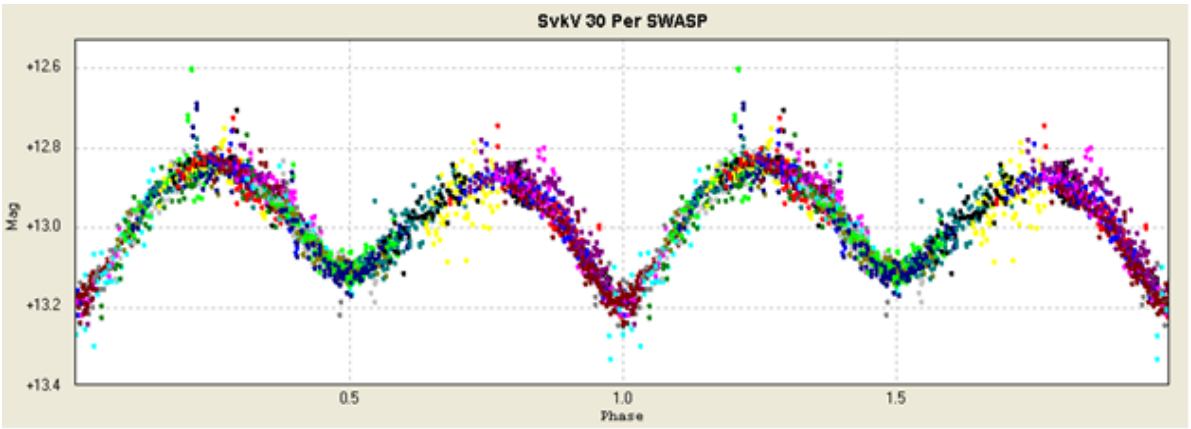

Figure 6: Phase diagram (light curve) for SvkV30 Per, data obtained from SuperWASP public archive.

Observations of SvkV31 Cas, SvkV32 Cas, SvkV43 Cas, SvkV44 Cas

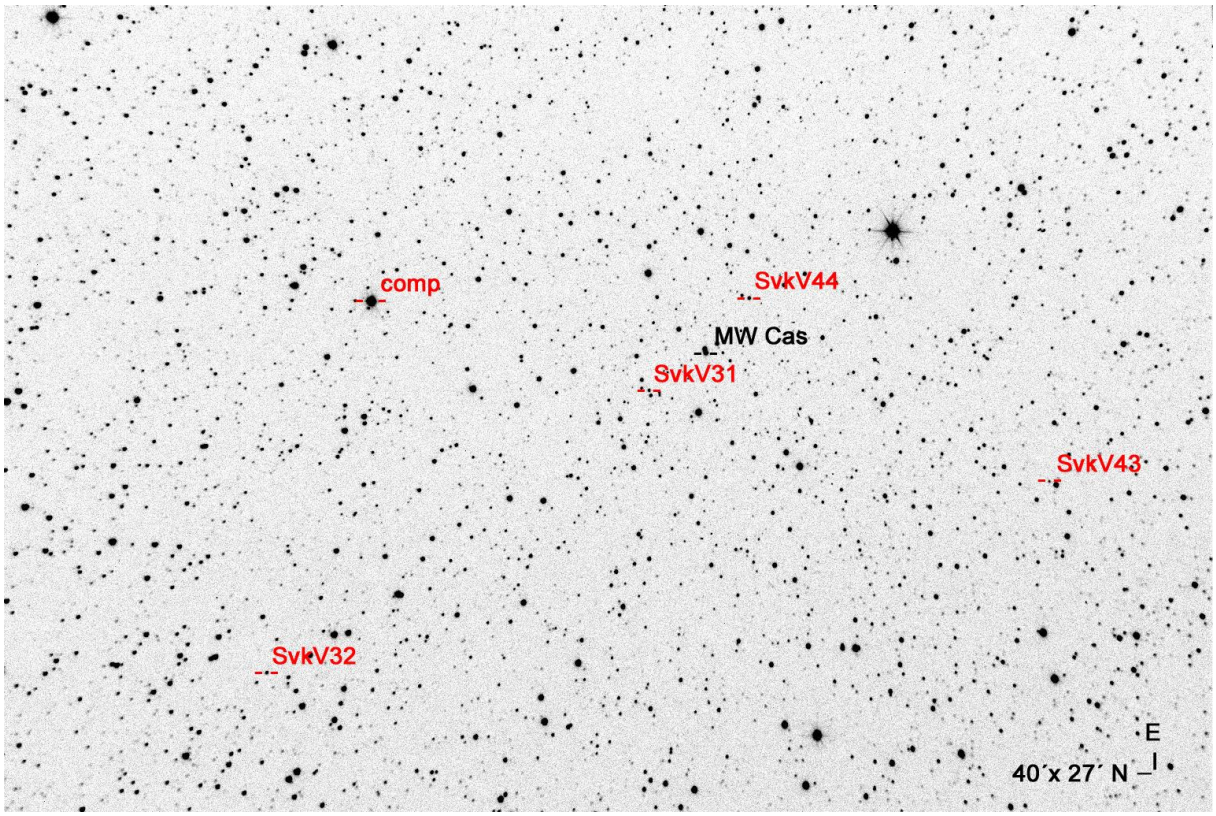

Figure 7: CCD picture of the variable stars SvkV31 Cas, SvkV32 Cas, SvkV43 Cas, SvkV44 Cas and the comparison star TYC 3657 1313.

SvkV31 Cas (*USNO B1.0 1451-0009950, R.A.= 001641.29 DEC.= +550652.84 Equinox: 2000.0*) (type EW, period 0,29718 day, brightness 15.28 (V) mag, amplitude 0.31 mag.)

SvkV31 Cas	T observed HJD	Error 1σ Bootstrapping	O - C	Minimum	observer
No.	d	±d	d	type	
Min1	2455826.32047	0.00052	0.0038	II	MV
Min2	2455826.46411	0.00033	-0.0012	I	MV
Min3	2455829.29322	0.00035	0.0047	II	MV
Min4	2455829.43685	0.00026	-0.0002	I	MV
Min5	2455830.32913	0.00027	0.0005	I	MV
Min6	2455830.48145	0.00030	0.0042	II	MV
Min7	2455852.47021	0.00036	0.0017	II	MV
Min8	2455852.31819	0.00064	-0.0018	I	MV
Min9	2455853.36180	0.00034	0.0017	II	MV
Min10	2455866.43550	0.00047	-0.0005	II	MV
Min11	2455867.32835	0.00041	0.0008	II	MV
Min12	2455868.21989	0.00054	0.0008	II	MV

Table 8: SvkV31 Cas, Times of minimum are given in HJD.

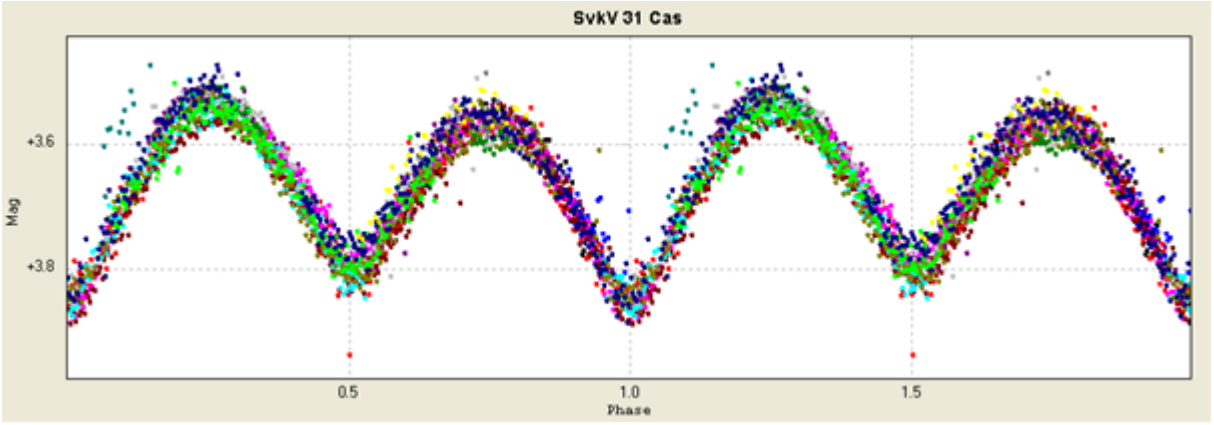

Figure 8: Phase diagram (light curve) for SvkV31 Cas, each colour represents another observation set.

SvkV32 Cas (*USNO B1.0 1453-0009166, R.A.= 001539.20 DEC.= +551930.08 Equinox: 2000.0*) (type EW, period 0.47740 day, brightness 15.60 (V) mag, amplitude 0.18 mag.)

SvkV32 Cas	T observed HJD	Error 1σ Bootstrapping	O - C	Minimum	observer
No.	d	±d	d	type	
Min1	2455828.41003	0.00050	-0.0004	I	MV
Min2	2455829.36319	0.00056	-0.0020	I	MV
Min3	2455830.31768	0.00057	-0.0023	I	MV
Min4	2455833.42352	0.00170	0.0007	II	MV

Table 9: SvkV32 Cas, Times of minimum are given in HJD.

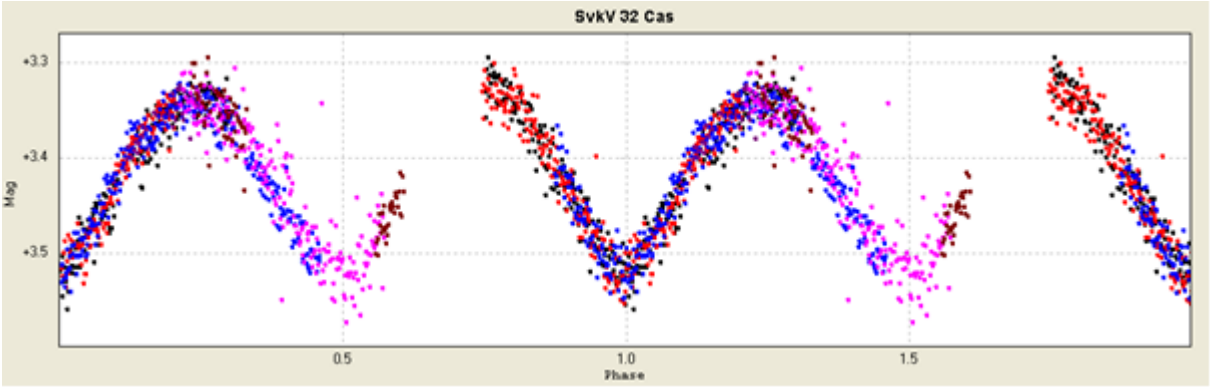

Figure 9: Phase diagram (light curve) for SvkV32 Cas, each colour represents another observation set.

SvkV43 Cas (*3UC290-006467, R.A.= 001618.37 DEC.= +545358.10 Equinox: 2000.0*)
(type EW, period 0.36642 day, brightness 16.51 (V) mag, amplitude 0.34 mag.)

SvkV43 Cas	T observed HJD	Error 1σ Bootstrapping	O - C	Minimum	observer
No.	d	±d	d	type	
Min1	2455826.43877	0.00111	-0.0004	I	MV
Min2	2455841.46428	0.00132	0.0019	I	MV
Min3	2455852.45820	0.00089	0.0032	I	MV
Min4	2455853.36995	0.00188	-0.0011	II	MV

Table 10: SvkV43 Cas, Times of minimum are given in HJD.

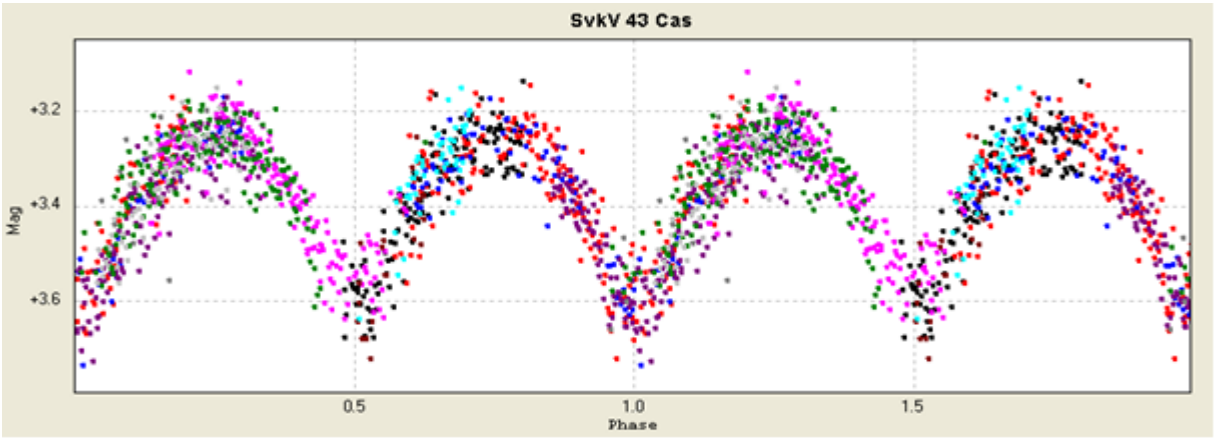

Figure 10: Phase diagram (light curve) for SvkV43 Cas, each colour represents another observation set.

SvkV44 Cas (*3UC291-006190, R.A.= 001701.59 DEC.= +550333.28 Equinox: 2000.0*)
(type EB, period 0,81994 day, brightness 14.58 (V) mag, amplitude 0.17 mag.)

SvkV44 Cas	T observed HJD	Error 1σ Bootstrapping	O - C	Minimum	observer
No.	d	±d	d	type	
Min1	2455829.39333	0.00133	0,0010	II	MV
Min2	2455868.33902	0.00096	-0,0004	I	MV

Table 11: SvkV44 Cas, Times of minimum are given in HJD.

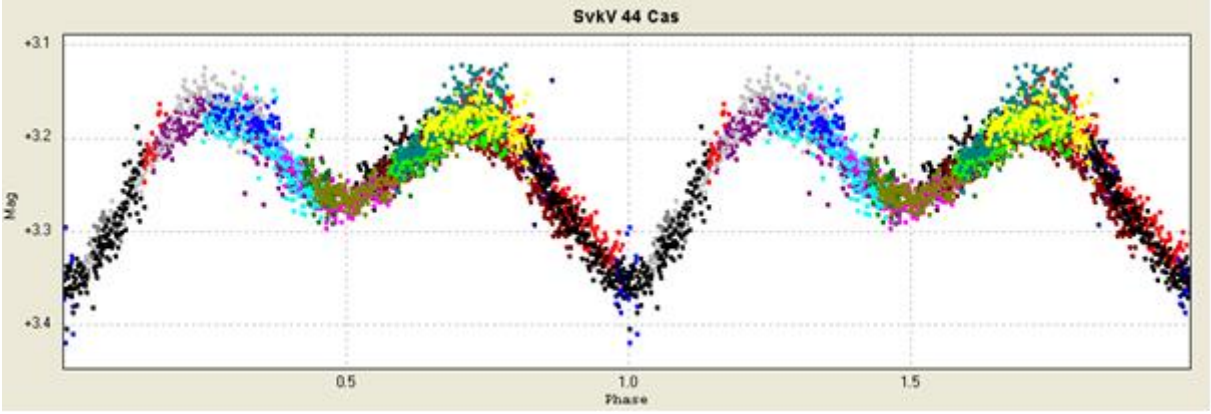

Figure 11: Phase diagram (light curve) for SvkV44 Cas, each colour represents another observation set.

Observations of SvkV35 And, SvkV36 And, SvkV37 And SvkV38 And

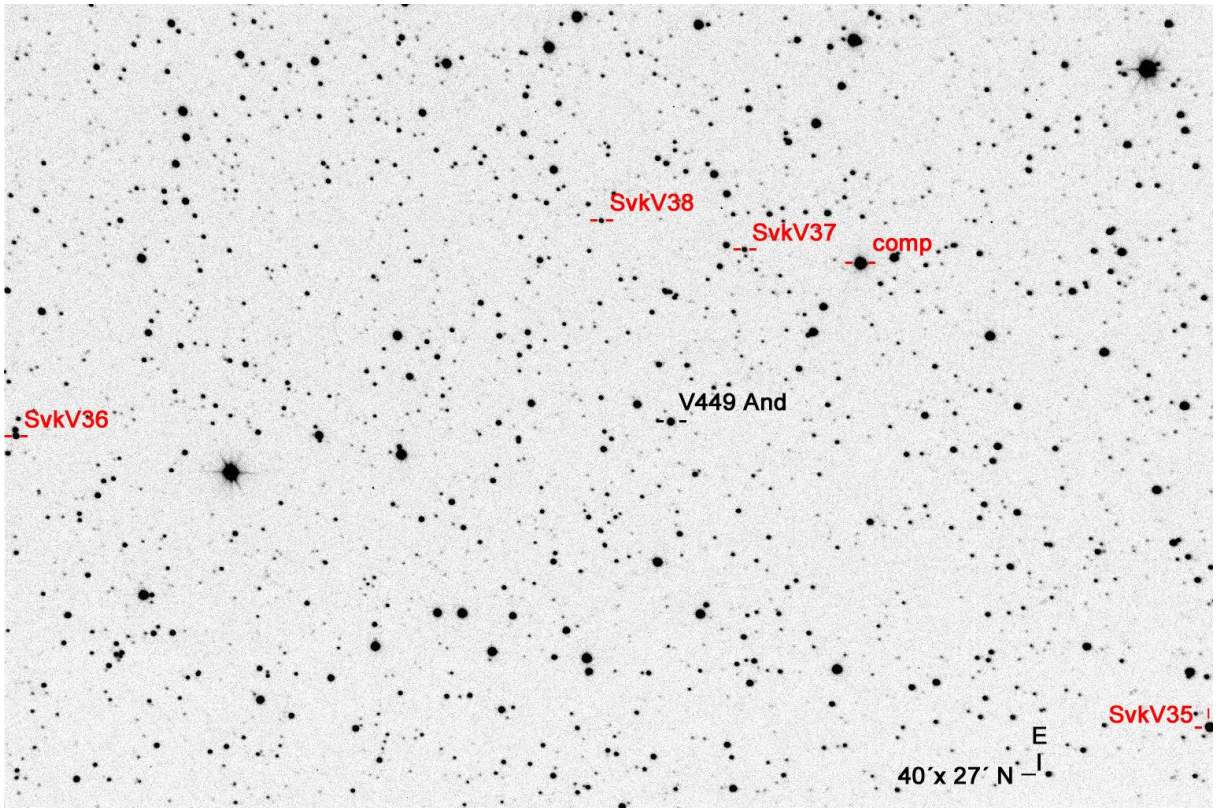

Figure 12: CCD picture of the variable stars SvkV35 And, SvkV36 And, SvkV37 And SvkV38 And and the comparison star TYC 3281 1988.

SvkV35 And (*TYC 3281-85, R.A.= 020846.33 DEC.= +462603.07 Equinox: 2000.0*)
(type EW, period 0.51782 day, brightness 11.43 (V) mag, amplitude 0.21 mag.)

SvkV35 And	T observed HJD	Error 1σ Bootstrapping	O - C	Minimum	observer
No.	d	±d	d	type	
Min1	2456154.52280	0.00098	0.0001	II	MV
Min2	2456155.55762	0.00073	-0.0007	II	MV
Min3	2456898.37440	0.00045	-0.0038	I	MV
Min4	2456957,40993	0,01930	-0.0003	I	MV

Table 12: SvkV35 And, Times of minimum are given in HJD.

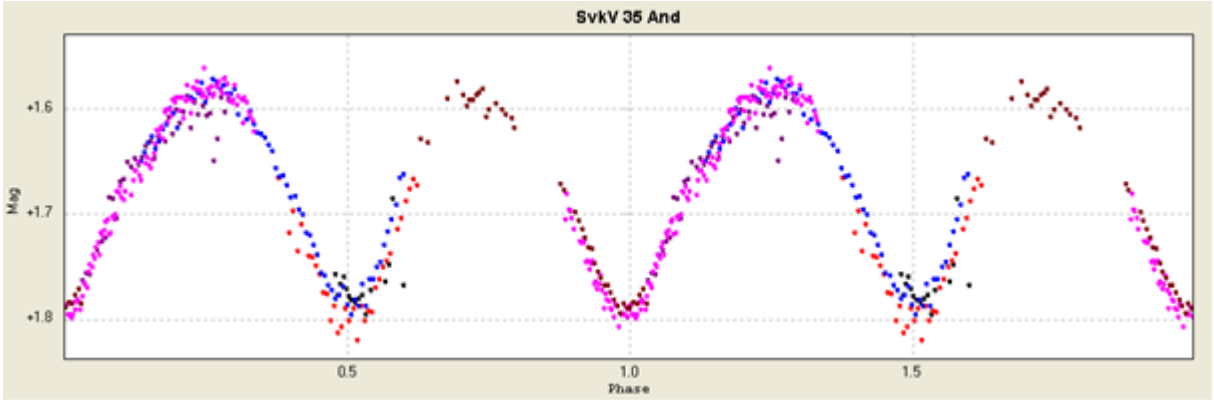

Figure 12: Phase diagram (light curve) for SvkV35 And, each colour represents another observation set.

SvkV36 And (*GSC 3285 1170, R.A.= 020947.52 DEC.= +470432.67 Equinox: 2000.0*)
(type EB, period 0.33766 day, brightness 13.02 (V) mag, amplitude 0.35 mag.)

SvkV36 And	T observed HJD	Error 1σ Bootstrapping	O - C	Minimum	observer
No.	d	±d	d	type	
Min1	2456154.55638	0.00073	0.0011	I	MV
Min2	2456155.40103	0.00105	0.0014	II	MV
Min3	2456155.56668	0.0007	-0.0016	I	MV
Min4	2456157.42895	0.00068	0.0033	II	MV
Min5	2456930.34091	0.00062	0.0001	I	MV
Min6	2456930.50902	0.00034	-0.0005	II	MV

Table 13: SvkV36 And, Times of minimum are given in HJD.

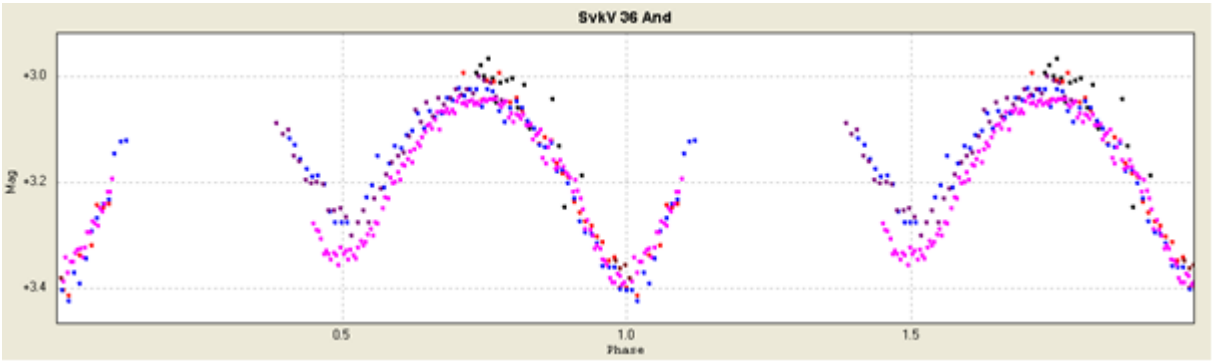

Figure 13: Phase diagram (light curve) for SvkV36 And, each color represents another observation set.

SvkV37 And (*USNO B1.0 1366-0046496, R.A.= 021019.07 DEC.= +464043.78 Equinox: 2000.0*)
(type EB, period 0.38298 day, brightness 14.21 (V) mag, amplitude 0.47 mag.)

SvkV37 And	T observed HJD	Error 1σ Bootstrapping	O - C	Minimum	observer
No.	d	±d	d	type	
Min1	2456155.54648	0.00113	-0.0004	I	MV
Min2	2456157.46287	0.00145	0.0011	I	MV
Min3	2456898.33162	0.00118	-0.0045	II	MV
Min4	2456898.52304	0.00040	-0.0050	I	MV
Min5	2456930.50311	0.00049	-0.0033	II	MV

Table 14: SvkV37 And, Times of minimum are given in HJD.

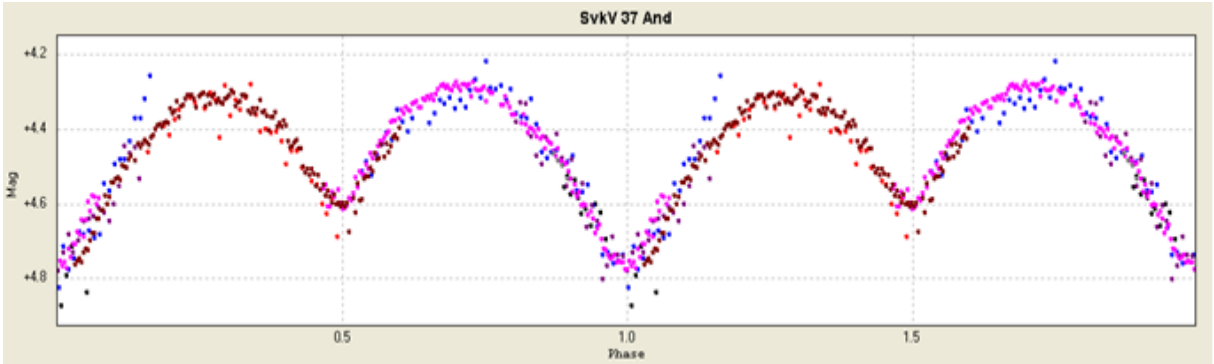

Figure 14: Phase diagram (light curve) for SvkV37 And, each color represents another observation set.

SvkV38 And (*USNO B1.0 1367-0045541, R.A.= 021025.37 DEC.= +464520.84 Equinox: 2000.0*)
(type EW, period 0.44394 day, brightness 14.72 (V) mag, amplitude 0.75 mag.)

SvkV38 And	T observed HJD	Error 1σ Bootstrapping	O - C	Minimum	observer
No.	d	±d	d	type	
Min1	2456155.52605	0.00090	-0.0016	I	MV
Min2	2456898.46764	0.00026	-0.0019	II	MV
Min3	2456930.43403	0.00033	0.0004	II	MV

Table 15: SvkV38 And, Times of minimum are given in HJD.

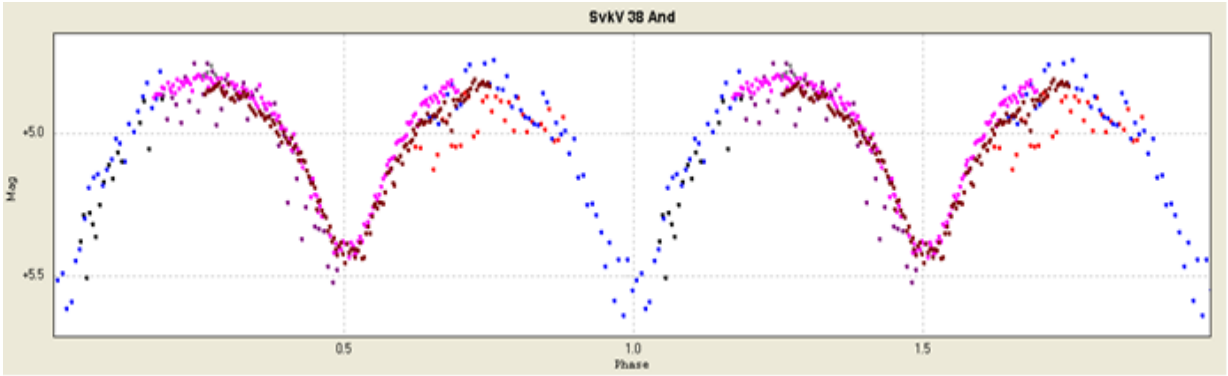

Figure 15: Phase diagram (light curve) for SvkV38 And, each colour represents another observation set.

Observations of SvkV41 Oph

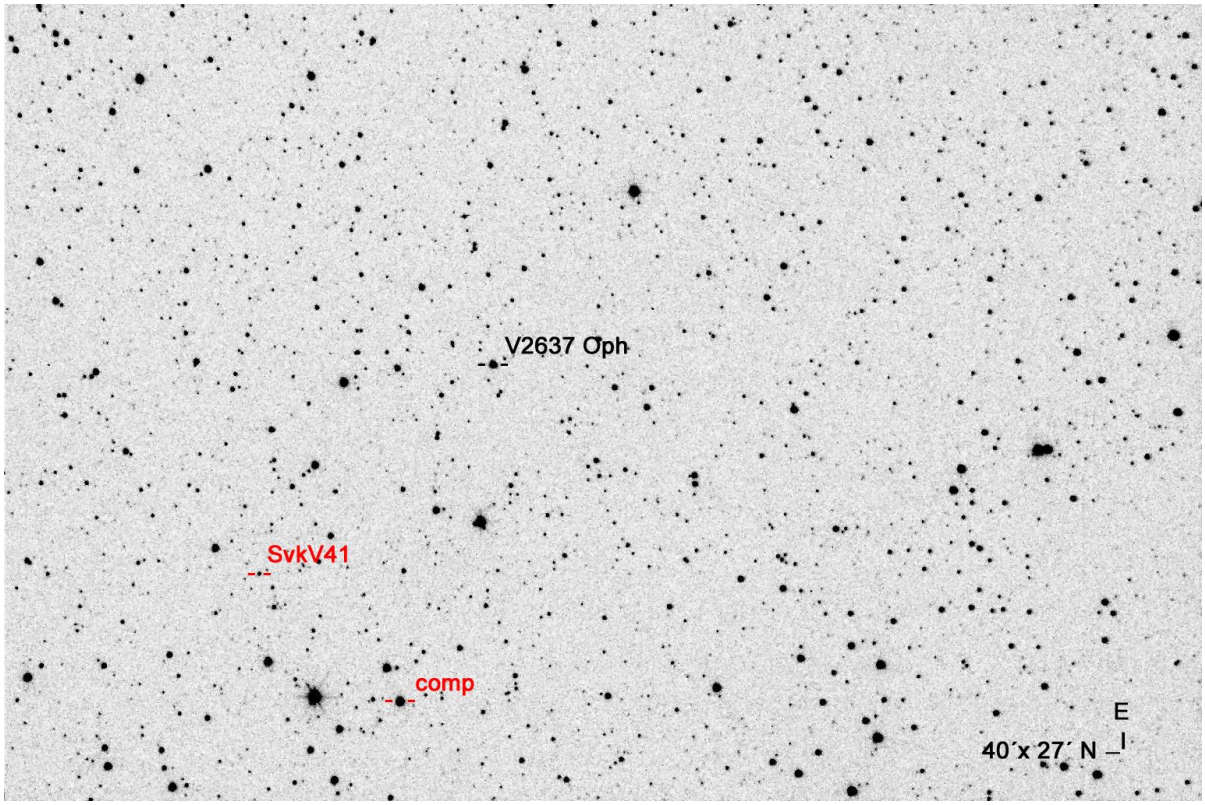

Figure 16: CCD picture of the variable star SvkV41 Oph and the comparison star TYC 408 507.

SvkV41 Oph (*USNO B1.0 0954-0288850, R.A.= 171803.43 DEC.= +052428.00 Equinox: 2000.0*)
(type EW, period 0,41127 day, brightness 14.90 (V) mag, amplitude 0.50 mag.)

SvkV 41 Oph	T observed HJD	Error 1σ Bootstrapping	O - C	Minimum	observer
No.	d	±d	d	type	
Min1	2456431.41392	0.00161	0.0039	I	MV

Table 16: SvkV41 Oph, Times of minimum are given in HJD.

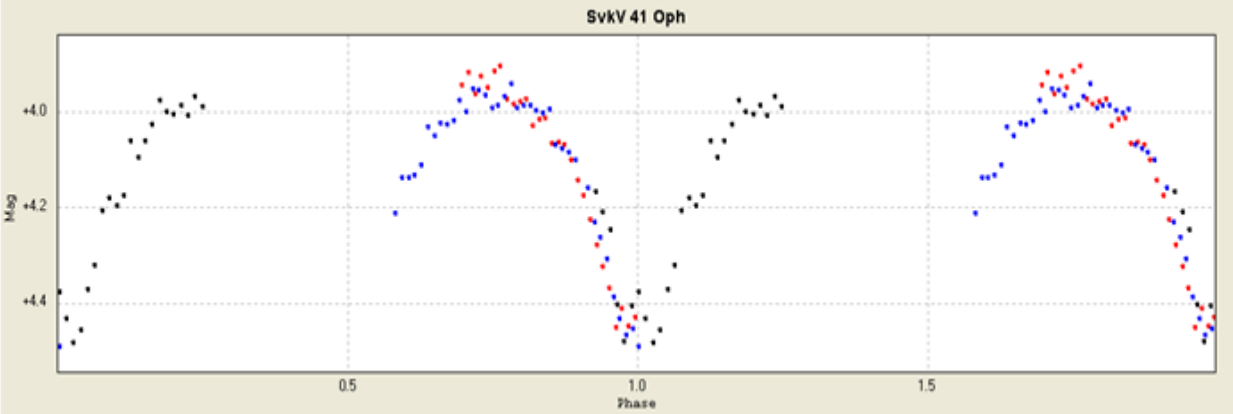

Figure 17: Phase diagram (light curve) for SvkV41 Oph, each colour represents another observation set.

Observations of SvkV42 Cyg

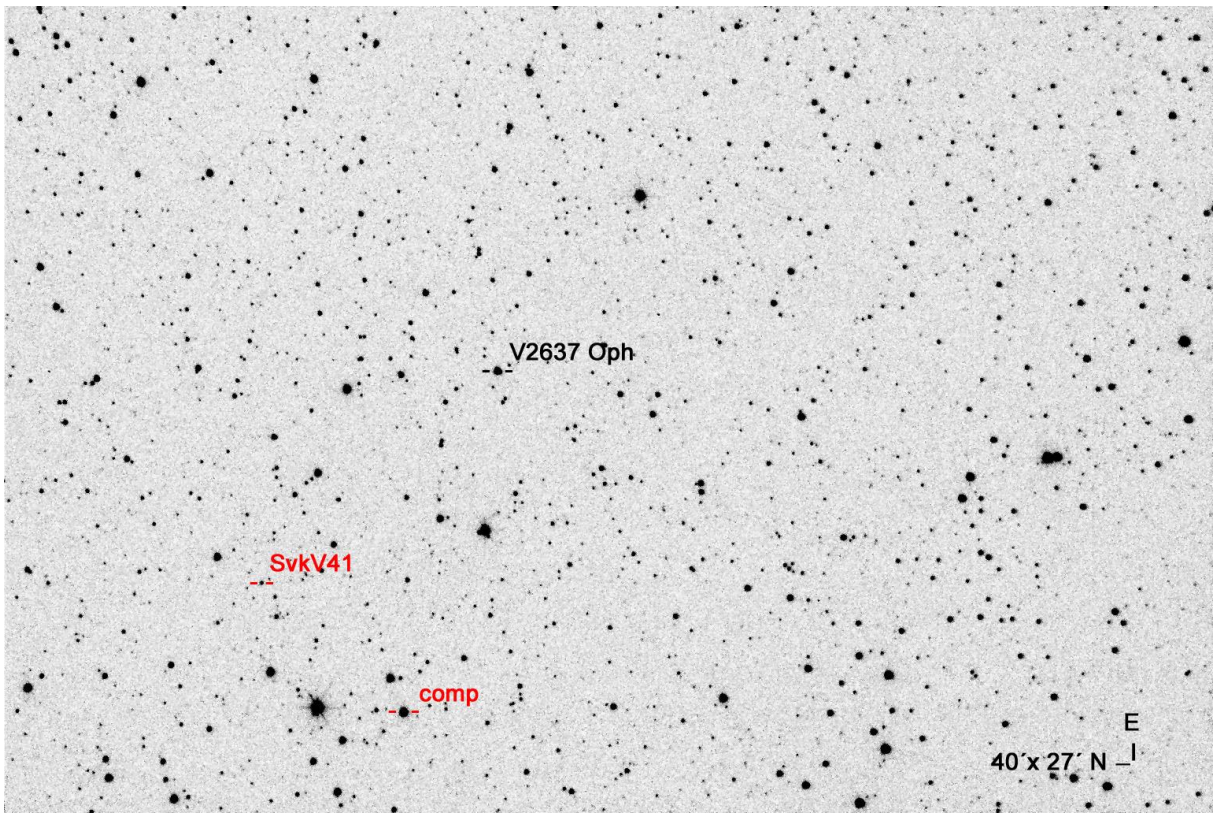

Figure 18: CCD picture of the variable star SvkV42 Cyg and the comparison star TYC 2137 2923.

SvkV42 Cyg (*3UC238-176140, R.A.= 192707.75 DEC.= +285849.54 Equinox: 2000.0*)
(type EW, period 0,45050 day, brightness 15.48 (V) mag, amplitude 0.30 mag.)

SvkV42 Cyg	T observed HJD	Error 1σ Bootstrapping	O - C	Minimum	observer
No.	d	±d	d	type	
Min1	2456461.40660	0.00116	0.0466	I	MV

Table 17: SvkV42 Cyg, Times of minimum are given in HJD.

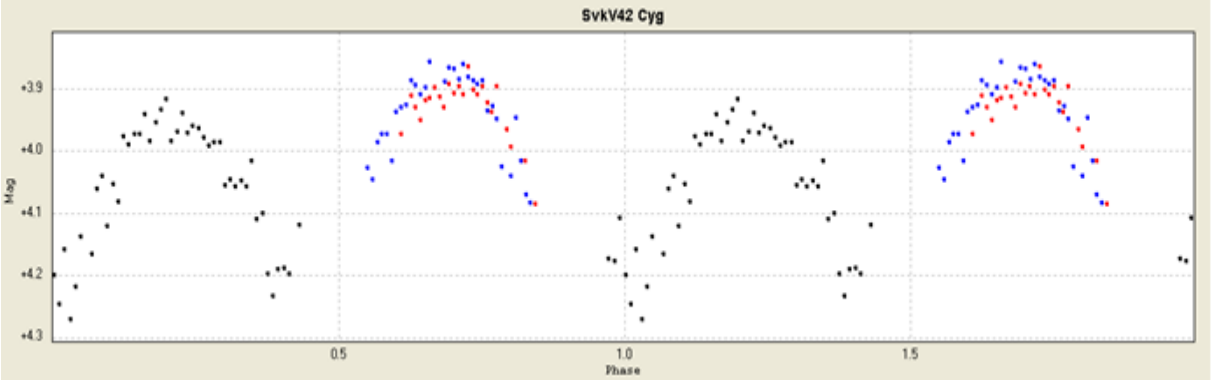

Figure 19: Phase diagram (light curve) for SvkV42 Cyg, each colour represents another observation set.

References

This paper makes use of data from the DR1 of the WASP data (Butters et al. 2010) as provided by the WASP consortium, and the computing and storage facilities at the CERIT Scientific Cloud, reg. no. CZ.1.05/3.2.00/08.0144 which is operated by Masaryk University, Czech Republic.

SuperWASP public archive, http://www.wasp.le.ac.uk/public/

Vanmunster T., 2011, Peranso V2.50, http://www.peranso.com/

Motl, D., 2006, MuniWin version 1.1.24, http://c-munipack.sourceforge.net/

GUIDE 9.0, http://www.projectpluto.com

Stetson, P.B., 1987, PASP 99, 191

Minima Timing of Eclipsing Binaries (Brát, Mikulášek, Pejcha 2012)

http://var2.astro.cz/library/1350745528_ebfit.pdf

An internet portal of Czech variable star researchers, http://var.astro.cz

OPEN EUROPEAN JOURNAL ON VARIABLE STARS
September 2014 http://var.astro.cz/oejv ISSN 1801-5964

Observing RR Lyrae type stars

M. SKARKA [1, 2], J. LIŠKA [1, 2], R. DŘEVĚNÝ [2, 3], R. F. AUER [2, 4]

(1) Department of Theoretical Physic and Astrophysics, Faculty of Science, Masaryk University, Kotlářská 2, 611 37 Brno Czech Republic, maska@physics.muni.cz
(2) Variable Star and Exoplanet Section of Czech Astronomical Society, Vsetínská 941/78, 757 01 Valašské Meziříčí, Czech Republic
(3) Znojmo observatory, Vinohrady 57, 669 02 Znojmo, Czech Republic
(4) South Moravian Observatory, Chudčice 273, 664 71, Czech Republic

Abstract: A current status of an ongoing survey dealing with observation of RR Lyrae type stars is presented. This project, called the Czech RR Lyrae observation project, works in cooperation with amateur observers, and aims to collect precise multicolour photometric data of bright RR Lyrae stars. The first important result was the discovery of the Blazhko effect in CN Cam.

Abstrakt: V tomto krátkém příspěvku je popsán současný status přehlídky zabývající se hvězdami typu RR Lyrae. Tento projekt, nazvaný the Czech RR Lyrae observation project, funguje ve spolupráci s amatérskými pozorovateli a má za cíl získávat přesná fotometrická data pro jasné hvězdy typu RR Lyrae v různých fotometrických barvách. Prvním důležitým výsledkem projektu byl objev Blažkova jevu u hvězdy CN Cam.

The project was introduced at the 43rd Conference on Variable Stars Research of the Czech astronomical society in 2011 when the first announcement for observers was released. At that moment, five observers were willing to join the project. Everything seemed to go well, the Blazhko effect in CN Cam was discovered (Skarka, Hoňková & Juryšek, 2013), and a few other targets were monitored. However, problems came with the year of 2013, when observations from Ostrava and Brno were stopped for almost two years and only one observer remained active in this period. Fortunately, other observers joined our group, and observations from Brno restarted in 2014.

The project, which was initially dedicated for observation of Blazhko stars and stars without good quality data in automatic surveys, was progressively extended to monitor bright RR Lyrae stars without other limitations. The currently refined aim of the project is the collection of precise multicolour photometry in BVR_cI_c filters for both Blazhko and regular RR Lyrae stars. This will lead to an extensive catalogue of light curves similar to the one of Lub (1977), which makes possible a refinement of light elements, determination of light curve characteristics, and description of modulation in many targets. In addition, data gathered in this survey will be useful for statistical studies of RR Lyrae stars. A similar survey, that was an inspiration for our project, took place between 2004 and 2013 in Hungary (e.g. Jurcsik et al., 2009).

The main advantage of the project compared to automated surveys is that we can measure many targets in different filters, say, simultaneously. Appropriate attention can be paid for exposure times, comparison stars selection, and time schedule of observations for each particular target to achieve the best possible precision. Since amateurs mainly use small-aperture telescopes of diameter between 20 and 30 cm, only stars with maximum light brighter than 12.5 mag are considered for monitoring. The targets are assigned to observers exclusively to avoid merging data from different devices. However, all data are calibrated to standard Johnson-Cousins system. Although the vast majority of targets have declination higher than 20°, starting this year also stars from the southern hemisphere are considered to be monitored with the FRAM telescope (Prouza et al., 2010)

To give a short summary of the achieved results we can highlight a three-year monitoring of two Blazhko stars, complete light curves for three other stars and incomplete light curves for several other targets. An example of data gathered in 2014 with a 35cm Schmidt-Cassegrain telescope at Observatory and Planetarium in Brno are in fig. 1. Any other observer, who is interested in the project, is warmly welcomed to join our group.

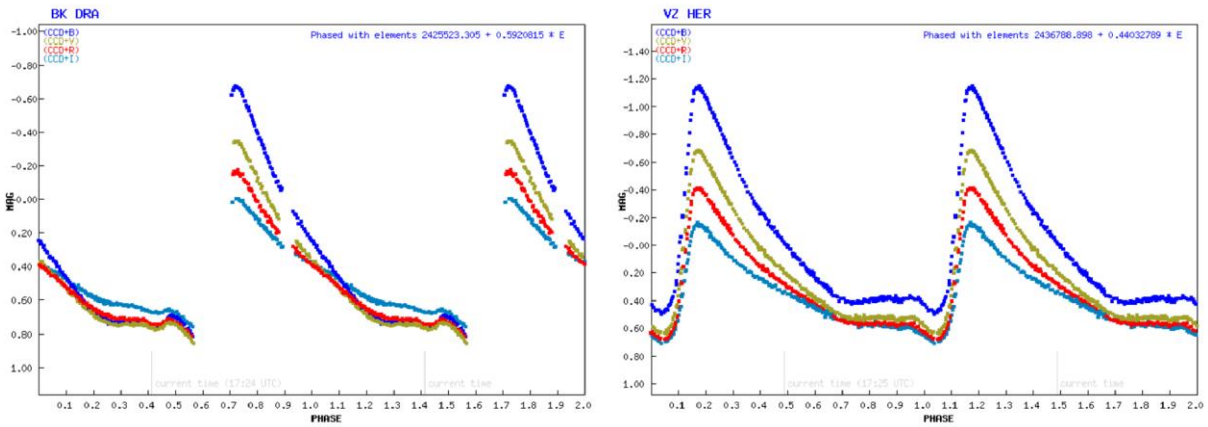

Figure 1: Light curves of BK Dra and VZ Her obtained in Brno in 2014.

Acknowledgements

Marek Skarka would like to express his deep gratitude to all observes interested in the project. The work on the survey has been financed by Masaryk University grant MUNI/A/0735/2012 and MUNI/A/0773/2013. The support of Brno Observatory and Planetarium is acknowledged.

References

Prouza, M., Jelínek, M., Kubánek, P., et al. 2010, Advances in Astronomy, 2010

Jurcsik, J., Sódor, Á., Szeidl, B. et al. 2009, MNRAS, 400, 1006

Lub, J. 1977, A&AS, 29, 345

Skarka, M., Hoňková, K. & Juryšek, J. 2013, IBVS, 6051, 1

OPEN EUROPEAN JOURNAL ON VARIABLE STARS
September 2014 http://var.astro.cz/oejv ISSN 1801-5964

O-C diagrams and period changes in stellar systems

J. LIŠKA [1], M. SKARKA [1]

(1) Department of Theoretical Physics and Astrophysics, Kotlářská 2, 611 37, Brno, Czech Republic, jiriliska@post.cz, maska@physics.muni.cz,

Abstract: Based on the visual inspection of all O-C diagrams available in the O-C gateway managed by the Variable stars and exoplanet section of the Czech astronomical society we present an overview of possible shapes of O-C diagrams together with discussion of possible effects causing such dependences. The nature of these effects is discussed for various types of periodic variable. We also give short remarks on interesting eclipsing systems BV Dra and BW Dra which form a visual pair and show antiparallel changes of their O-C diagrams. In addition we comment on period changes of UU Cam, and argue that it probably shows long-term Light Time Effect (LiTE) rather than sudden period change. Effects which are observable only in ultra-precise, quasi-continual measurements gathered by the *Kepler* satellite are discussed at the end of this contribution.

Abstrakt: Na základě vizuální prohlídky všech O-C diagramů dostupných v O-C bráně spravované Sekcí proměnných hvězd a exoplanet České astronomické společnosti, přinášíme přehled možných tvarů O-C diagramů společně s diskuzí možných efektů způsobujících právě takovéto závislosti. Povaha těchto efektů je diskutována pro odlišné typy periodicky proměnných hvězd. Také uvádíme krátké poznámky k zajímavým zákrytovým systémům BV Dra a BW Dra, které tvoří vizuální dvojhvězdu a vykazují antiparalelní změny v jejich O-C diagramech. Dále se zabýváme změnou periody dvojhvězdy UU Cam, která pravděpodobně vykazuje dlouhodobější efekt rozdílné dráhy LiTE než náhlou změnu v periodě. Efekty, které jsou pozorovatelné pouze v ultra přesných kvazi-kontinuálních měřeních získaných satelitem *Kepler* jsou diskutovány na konci tohoto příspěvku.

We performed visual inspection of all O-C diagrams for eclipsing binary systems available in O-C gateway managed by the Variable star and exoplanet section of the Czech astronomical society (Paschke & Brát 2006) during spring 2010. Basic effects influencing the shape of O-C diagram and their combination known from literature (e.g. Zejda et al. 1994, Mikulášek & Zejda 2013) were identified in many cases. Nevertheless, fine changes in O-C could be studied in detail only via high-accurate observations gathered by space projects such as the *Kepler* telescope (discussed at the end of this contribution).

Various effects can produce visually the same variations in O-C for different classes of periodic variables with different nature of light changes. For example, changes of orbital periods in eclipsing binaries (EBs) can produce the same O-C diagram as changes in pulsation periods of pulsating stars (PSs), or in rotational periods of CP stars, pulsars etc. Observed O-C diagrams (favoring EBs) can be divided into several basic classes according to their shapes. Observed examples of these classes from the O-C gateway are shown in Fig. 1 and Fig. 2. These effects are better pronounced when synthetic models of O-C diagrams (Fig. 3) were calculated. These models were supplemented with randomly generated values with small dispersion to simulate real measurements.

(1) **Horizontal line with average O-C = 0.0** (Fig. 1a, 3a) – correct value of constant period with correct value of zero epoch

(2) **Horizontal line with average O-C ≠ 0.0** (Fig. 3b) – correct value of constant period with inaccurate value of zero epoch

(3) **Oblique line** (Fig. 3c) – constant period with inaccurate value of period

(4) **Double horizontal line** (primary minima have average O-C = 0.0, secondary minima O-C ≠ 0.0 (Fig. 1b, 3d) – constant period, eclipsing system has an eccentric orbit

(5) **Parabolic (cubic) shape** – period lengthening (Fig. 1c, 3e) or shortening (Fig. 1d, 3f) caused by mass transfer in EBs, mass loss, radiation of gravitational waves (two high-gravitationally interacting objects in small distance e.g. neutron stars), evolutionary effects, small part of LiTE imitating parabola, etc.

(6) **Strictly periodic variations** caused by gravitational influence of an additional body in the system (third body in EBs, second body in PSs) – Light Time (Travel) Effect (*LiTE*). In EBs primary and secondary minima vary in the same phase (Fig. 2a, 3g). Periodic variations can also be produced by the Blazhko effect in PSs (RR Lyraes, cepheids).

(7) **Strictly periodic variations** when primary and secondary minima of EBs vary in the anti-phase (Fig. 2b, 3h) – apsidal motion in EBs with an eccentric orbit

(8) **Periodic variations with modulation** of the shape (Fig. 3i) – result of an eccentric orbit of the additional component (source of LiTE) influenced by an apsidal motion, LiTE together with other effects

(9) **Other cyclic variations** (quazi-periodic O-C with changing amplitude) (Fig. 3j) – influence of magnetic field (EBs - Applegate mechanism), also in PSs and CP stars

(10) **Irregular variations, predictable** – gravitational influence of the third, fourth and other components (EBs)

(11) **Chaotic and random variations, unpredictable** (Fig. 2c, 3k) – result of random/chaotic effects, e.g. mass-transfer in cataclysmic variables (from donor component to a degenerate component through an accretion disc), random occurrence of surface spots on active stars (light changes influence extrema timings), pulsations in one of the components (also influence extrema timings), sudden changes in the internal structure of stars, instrumental artifacts, some kind of systematic errors etc.

(12) **Break in period** (Fig. 2d, 3l) – some strong changes in the system (e.g. collision with other star), very often part of LiTE (EBs) or combination of several effects, changes in inferior of stars, some kind of systematic errors etc.

(13) **Arbitrary combination or multiplication of mentioned effects** (EBs, PSs) – 2×LiTE (Fig. 2f, 3m), LiTE and period lengthening (Fig. 2e, 3n), apsidal motion of EB + LiTE caused by the third body (Fig. 3o)

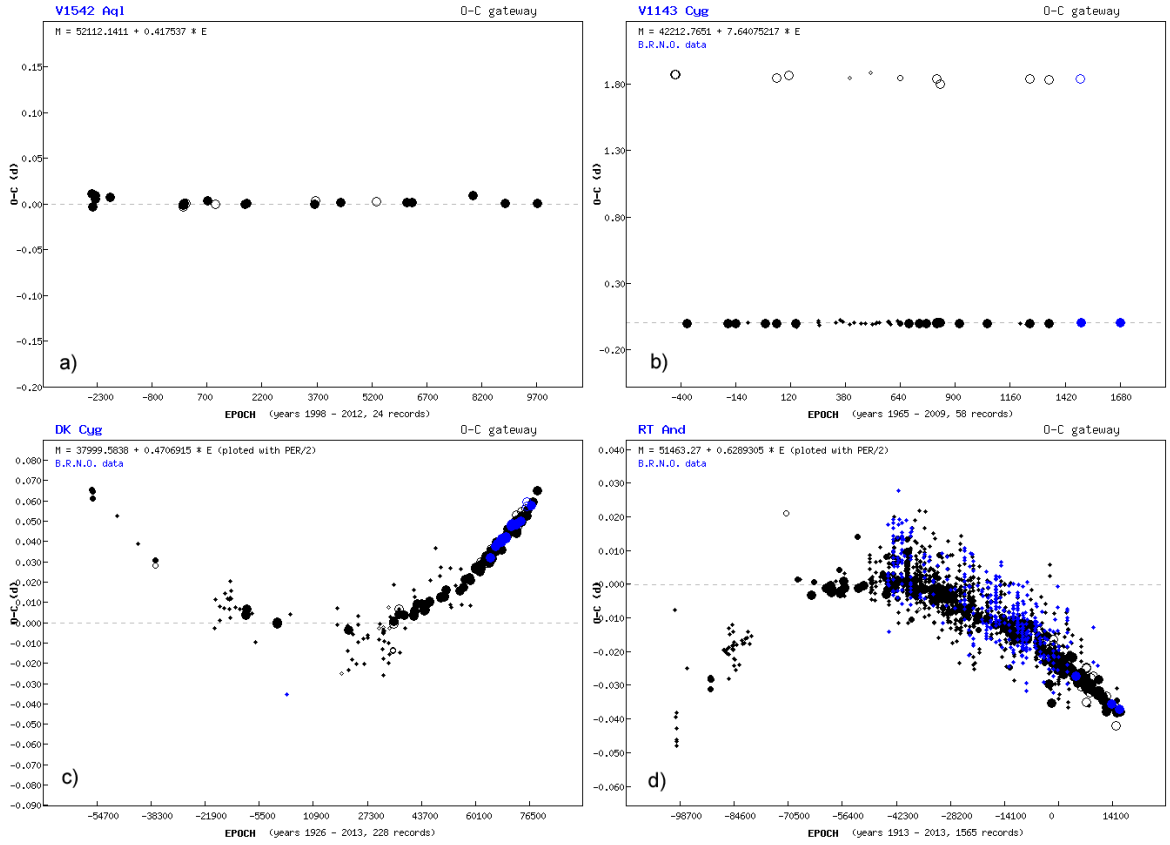

Figure 1: Examples of different O-C diagrams taken from the O-C gateway which are discussed in the text. Panels show the situation with constant period (a), constant period in eccentric system (b), period lengthening (c), and period shortening (d).

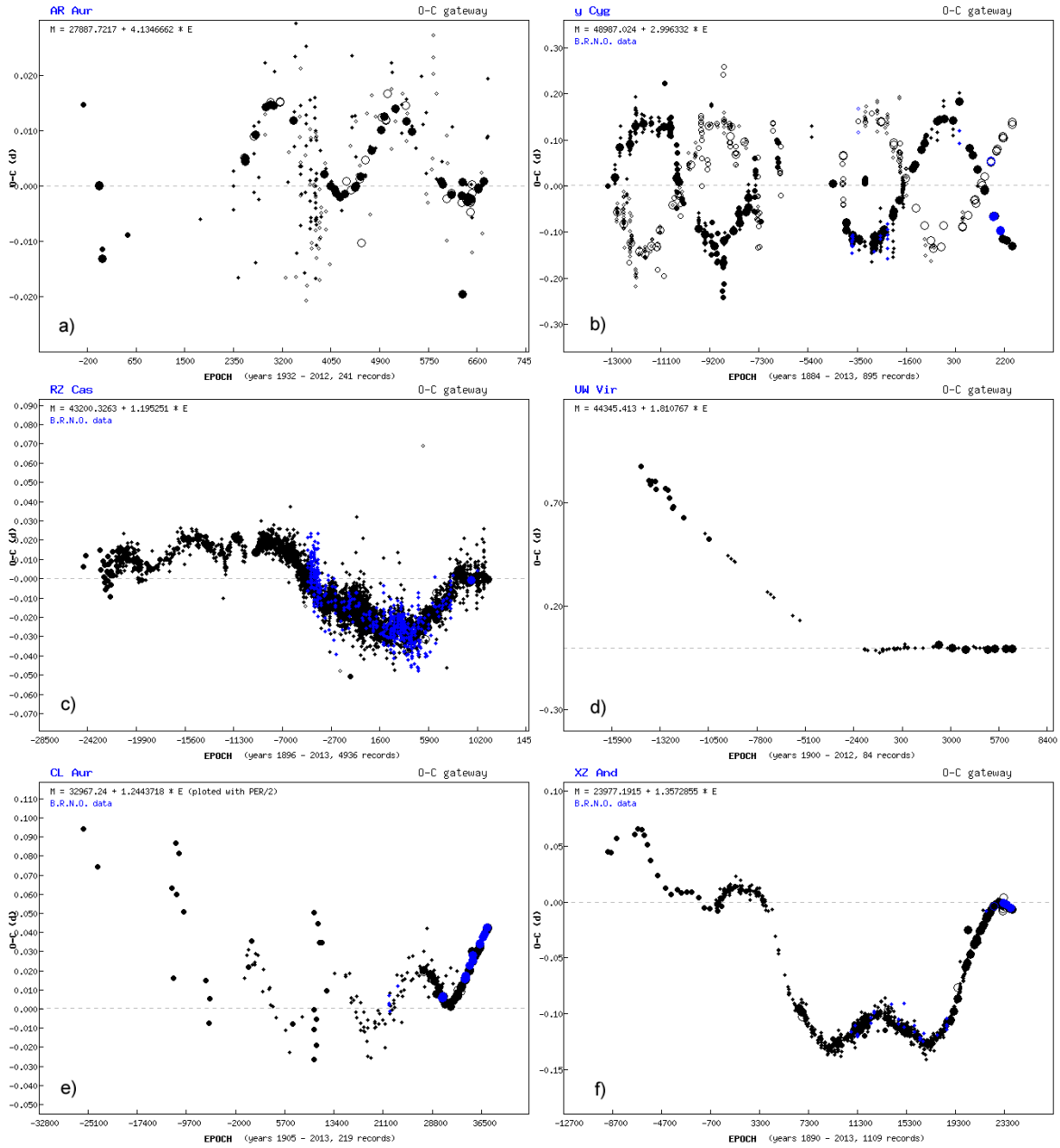

Figure 2: Examples of additional O-C diagrams taken from the O-C gateway which are discussed in the text. Panel a) shows the LiTE, panel b) shows the apsidal motion in an eccentric system, c) shows the chaotic and random changes, in panel d) the break in period is shown, combination of LiTE with period lengthening is plotted in panel e), and multiplication of LiTE is drawn in panel f).

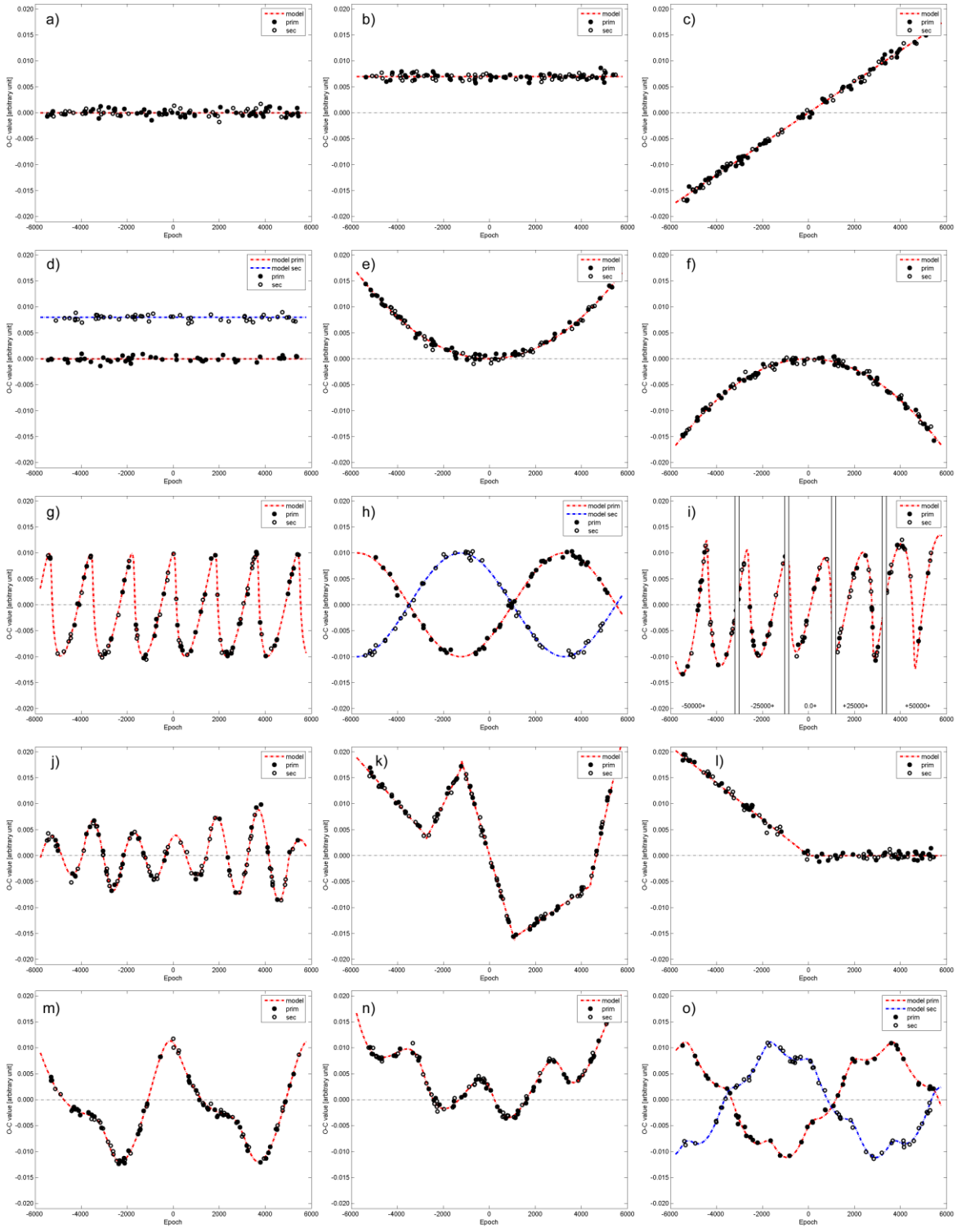

Figure 3: Synthetic models of O-C diagrams discussed in the text. High accurate models are supplemented with randomly generated values with small dispersion simulating real measurements. Panels show the situation with constant period (a), the constant period with wrong value of zero epoch (b), the constant period with its wrong value (c), the constant period in eccentric system (d), the period lengthening (e), the period shortening (f), the LiTE (g), the apsidal motion in an eccentric system (h), the LiTE caused by the third body on an eccentric orbit with apsidal motion (i), other cyclic changes (j), chaotic unpredictable variations (k), the break in period (l), the multiplication of two LiTEs (m), the combination of LiTE with period lengthening (n), the combination of apsidal motion of eccentric binary system and LiTE caused by third body (o).

BV Dra and BW Dra – visual pair of EBs with antiparallel O-C changes

BV Dra (HD 135421, R.A. = $15^h11^m50^s.36$, DEC. = +61°51'25".3, Equinox: 2000.0, EW/KW type, period 0.3500671 day, brightness variation 7.88 – 8.48 mag (V), from VSX) and BW Dra (HIP 74368, R.A. = $15^h11^m50^s.11$, DEC. = +61°51'41".3, Equinox: 2000.0, EW/KW type, period 0.2921671 day, brightness variation 8.61 – 9.08 mag (V), from VSX) are both contact eclipsing binaries, which are in a small mutual angular distance of only about 16 arcsec. Both systems have similar proper motions and parallaxes (0.014(2) mas and 0.013(4) mas for BV and BW Dra, respectively) (van Leeuwen 2007), and also similar systematic radial velocities (Batten & Lu 1986). They form visual binary ADS 9537, which is a physically bounded quadruple system. This assumption is underlined by a ratio of their orbital periods (~ 0.35 d and ~ 0.29 d) which is close to small integer numbers 6:5. Batten & Lu (1986) estimated separation of the two systems about 1150 AU and also orbital period of about 22 000 years. O-C diagrams of both systems have similar shapes but changes are in antiphase (Fig. 4). We suggest a very simple explanation of this behavior – effects resulting from the change of the orbital periods are for the both systems the same – the LiTE (system BV Dra causes LiTE for BW Dra and vice versa). Actual amplitude of O-C variations (0.01 d and 0.07 d for BV and BW Dra, respectively) is not in conflict with our assumption, because the total amplitude of LiTE based on their separation 1150 AU is at least 6.6 d. The smaller amplitude of O-C changes is correct in more massive system BV Dra. From the both O-C shapes we can estimate that both systems were probably in maximal mutual radial distance approximately in year 1997 (a gap in O-C diagram BW Dra is from 1991 to 2003, similarly for BV Dra). Nevertheless, orbital period of the quadruple system BV Dra–BW Dra is too long, and probability that they are in maximal radial distance just in this century is very low. Maybe another effects such as mutual gravitational disturbation in quadruple system or magnetohydrodynamic effects could play a role. Combined analysis of astrometric variations in position of both systems and LiTEs from O-C diagrams together with radial velocity variations would certainly shed some light on this problem.

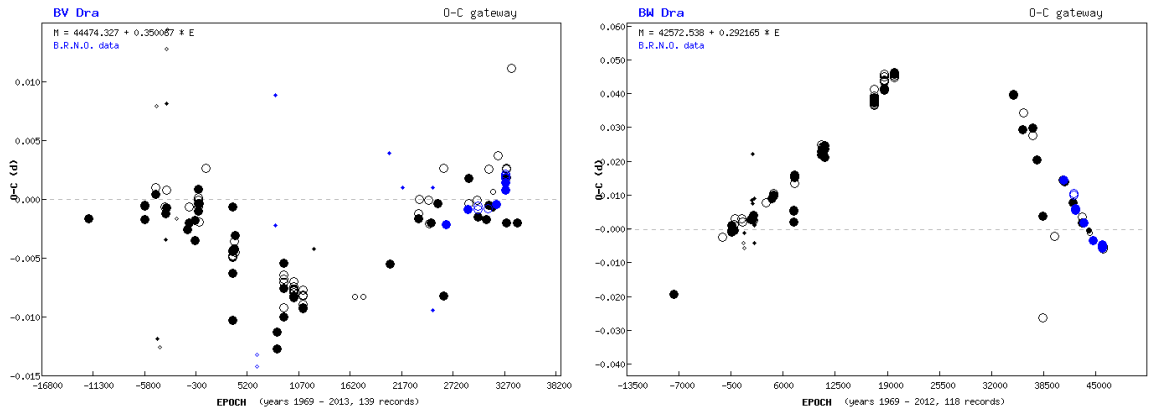

Figure 4: O-C diagrams for the quadruple system consisting of two eclipsing binary systems BV Dra (left) and BW Dra (right), which creates a visual binary with actual angular distance of about 16 arcsec. The shapes of O-Cs suggest LiTE mimicking as a break in period or deformed parabola.

UU Cam – another system with possible LiTE

The shape of the O-C diagram of UU Cam (GSC 04339-00474, RA = $03^h52^m17^s.70$, DEC = +74°33'56".5, Equinox: 2000.0, EW type, period 0.682544 day, brightness variation 11.40 – 11.90 mag (V), from VSX) indicates rapid and irregular changes in orbital period of the system (Fig. 5, left). We tested different values of the period and it was found that the period was 0.682529(2) d till 1969 and about 30 years later it was about 0.682557(1) d. It indicates either the break in period or LiTE caused by possible third body in the system (Fig. 5, right). For our prefer LiTE explanation, we visually estimated ephemeris of eclipses

$$T_{\min} = 2446360.12 + 0.6825405 \times E,$$

and possible orbital period of the third body with length of about 80 years (the whole interval of observations) or more. The semi-amplitude of LiTE could be about 0.12 light days. It is important to note, that the system was classified as an RR Lyrae type pulsating star for a long time, and thus detailed re-analysis mainly of the old measurements would be suitable.

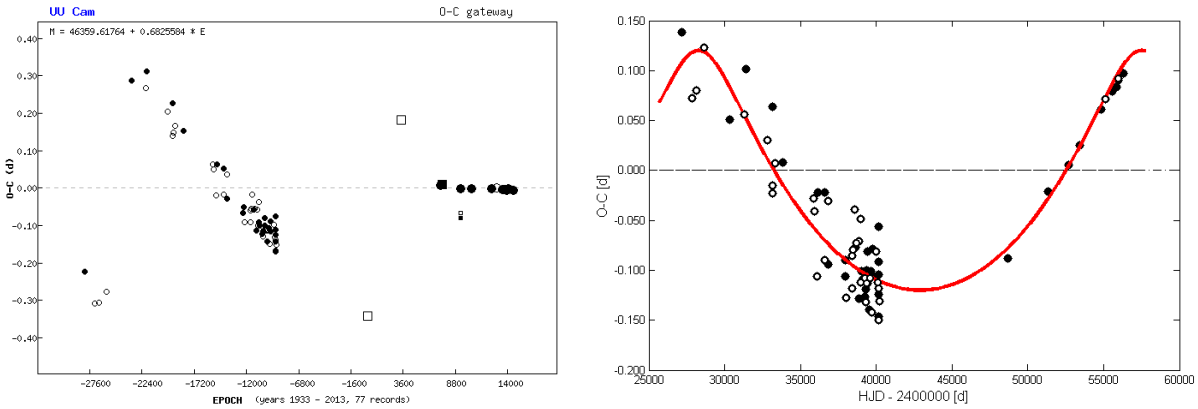

Figure 5: O-C diagram of the contact system UU Cam with original elements from the O-C gateway (left) and with our visually estimated elements which suppose the LiTE scenario with 80 year period (right).

The *Kepler* project and its impact on LiTE in eclipsing binary stars

High-accurate photometric measurements obtained by the *Kepler* satellite brought many discoveries which will have a major impact on stellar astrophysics in decades to come. The same field of view (FOV) with approximately 105 square-degrees in Cygnus-Lyrae region was continuously observed for about 4 years.

Originally only 383 EBs were cataloged in pre-launch *Kepler* target list compiled by Prša et al. (2011). The first results based on *Kepler* measurements resulted from its first 44-days run were published in the same paper by Prša et al. (2011). This catalogue contains ephemeris, morphology type and basic parameters determined from the light curve solution for 1879 EBs. Analysis of the data of 2165 EBs supplemented with additional measurements (total duration 125 days) were used for more accurate determination of the basic parameters by Slawson et al. (2011). In addition, they reconstructed Eclipsing Time Variations (ETV), which is the same as O-C diagram, to study the orbital period stability. They found 8 systems which clearly show signs of the third component manifesting itself as LiTE. In addition, they found additional tertiary eclipses (Fig. 6) in 4 EBs which would be hardly detectable in sparse, ground-based observations.

An overall analysis of ETV in the *Kepler* FOV was published by Conroy et al. (2014). They focused only on short-periodic systems, and therefore mainly on close binaries (subsample of 1279 objects from the total of 2605 EBs in the whole *Kepler* FOV). 236 binaries from this subsample (about 20 %) show signs of the third body. An analysis of the long period binaries will be published in the near future. At the conference Living Together: Planets, Host Stars and Binaries in Litomyšl, Orosz (2014), among others, presented that many of long-period EBs show variations in depth of minima which are caused probably by tidal friction and the Kozai (Kozai-Lidov) mechanism. Before the *Kepler* mission these tiny effects affecting the depths and shapes of eclipses were known only for several EBs.

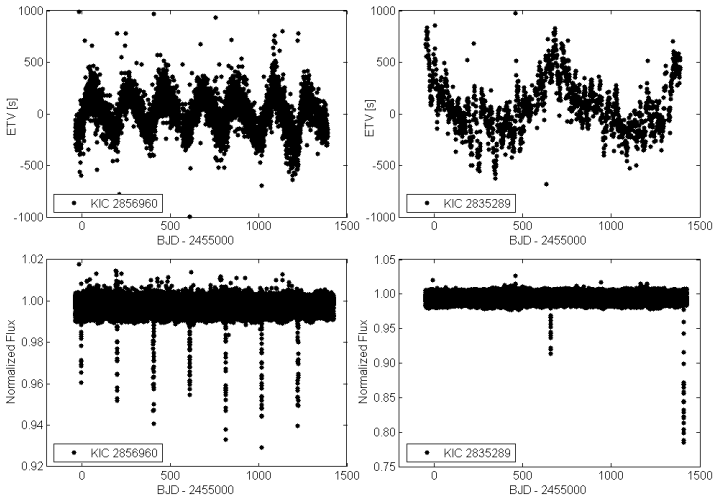

Figure 6: Two examples of ETV influenced by the third component (LiTE) which caused tertiary eclipses detected in phases of maximal or minimal values of ETV. System KIC 2856960 has a LiTE period P_3 = 204.5(1) d (left) and KIC 2835289 P_3 = 747.4(23.7) d (right). Data and looks of the graphs were adopted from Conroy et al. (2014).

Acknowledgements

The work was supported by Masaryk University grant MUNI/A/0930/2013. We would like to thank people who manage the O-C gateway for their great work on this database, namely Anton Paschke, Luboš Brát and Miloslav Zejda. Special thanks belong to all observers for their great job.

References

Batten, A. H. & Lu, W., 1986, PASP, 98, 92

Conroy, K. E., Prša, A., Stassun, K. G., et al, 2014, AJ, 147, 45

Mikulášek, Z. & Zejda, M., 2013, Úvod do studia proměnných hvězd, Masarykova univerzita, muni PRESS, Brno

Orosz, J. A., 2014, Invited talk in Living Together: Planets, Host Stars and Binaries, conference in Litomyšl

Paschke, A. & Brát, L., 2006, OEJV, 23, 13

Prša, A., Batalha, N., Slawson, R. W., et al., 2011, AJ, 141, 83

Slawson, R. W., Prša, A., Welsh, W. F., et al., 2011, AJ, 142, 160

van Leeuwen, F., 2007, A&A, 474, 653

Zejda, M., Borovička, J., Hájek, P., et al., 1994, Pozorování proměnných hvězd, Contributions of the Public Observatory and Planetarium in Brno, Volume 30